Tracking Control for Underwater Vehicle-Manipulator Systems with Velocity Estimation

Gianluca Antonelli, Fabrizio Caccavale, Stefano Chiaverini, and Luigi Villani

***Abstract*—In this paper, the problem of tracking a desired motion trajectory for an underwater vehicle-manipulator system without using direct velocity feedback is addressed. For this purpose, an observer is adopted to provide estimation of the system's velocity needed by a tracking control law. The combined controller-observer scheme is designed so as to achieve exponential convergence to zero of both motion tracking and estimation errors. In order to avoid representation singularities of the orientation, unit quaternions are used to express the vehicle attitude. Implementation issues are also considered and simplified control laws are suggested, aimed at suitably trading off tracking performance against reduced computational load. Simulation case studies are carried out to show the effectiveness of the proposed controller-observer algorithm. The obtained performance is compared to that achieved with a control scheme in which the velocity is reconstructed via numerical differentiation of position measurements. The results confirm that the chattering on the control commands is significantly reduced when the controller-observer strategy is adopted in lieu of raw numerical differentiation; this leads to lower energy consumption at the actuators and increases their lifetime.**

***Index Terms*—Manipulators, motion control, observers, tracking, underwater vehicles.**

I. Introduction

UNDERWATER tasks involving an autonomous vehicle equipped with a manipulator give rise to challenging control problems involving nonlinear, coupled, and high-dimensional systems. As typical in robotics, the execution of such tasks can be formulated in terms of a control problem regarding the manipulator's end-effector motion, for which several techniques have been proposed.

In recent years, advanced control techniques have been developed for autonomous underwater vehicles (AUV's) and remotely operated vehicles (ROV's), aimed at improving the capability of tracking desired position and attitude trajectories. Improvement of tracking performance typically requires control schemes based on the knowledge of the system's dynamics (i.e., inverse dynamics control laws, feedforward compensation), e.g., as in [1], [2], or based on adaptive actions [3]. However, as is typical in feedback control systems, the achievable performance is highly dependent on the accuracy of sensor measurements.

Manuscript received November 17, 1998; revised August 18, 1999.

G. Antonelli and S. Chiaverini are with the Dipartimento di Automazione, Elettromagnetismo, Ingegneria dell'Informazione e Matematica Industriale, Università degli Studi di Cassino, 03043 Cassino, Italy.

F. Caccavale and L. Villani are with the Dipartimento di Informatica e Sistemistica, Università degli Studi di Napoli Federico II, 80125 Napoli, Italy.

Publisher Item Identifier S 0364-9059(00)06688-7.

Subsea vehicles are typically equipped with acoustic sensors or video systems for position measurements, while the vehicle attitude can be obtained from gyroscopic sensors and/or compasses. Velocity measurements are usually obtained from sensors based on the Doppler effect.

Consider the case of an underwater vehicle-manipulator system (UVMS) involved in a manipulation task to be accomplished with high accuracy, i.e., the end-effector reference trajectories have to be tracked with small errors. Examples of such tasks are maintenance of off-shore structures and the recovery of materials on the sea bottom. Under these operating conditions, the vehicle's velocity is usually lower than typical cruising velocities. In order to achieve good tracking during the fulfilment of the task, accurate position and orientation measurements must be available at a relatively high update rate: this can be achieved, e.g., if the system is equipped with a vision-based sensing device. Moreover, the availability of accurate and noise-free velocity measurements is crucial for achieving the desired performance. Unfortunately, this is not guaranteed by Doppler effect sensors and sonars, especially during slow maneuvers. As a matter of fact, numerical differentiation of noisy position/orientation measurements leads to chattering of the control inputs, which may become unacceptable when quantization effects are present. Such phenomena lead to high-energy consumption at the actuators, and thus tend to reduce their lifetime and increase the failures rate. On the other hand, the use of low-pass filters on the numerically reconstructed velocities could deteriorate the overall tracking performance; in addition, since the system to be controlled is nonlinear, tuning of the filter parameters guaranteeing closed-loop stability is not straightforward and can be achieved only by a trial-and-error procedure.

Hence, it is worth devising algorithms for position and attitude control which do not require direct velocity feedback. This can be achieved by adopting a velocity observer which performs a nonlinear filtering of the measures from the position/orientation sensors and gives a noise-free estimation of the velocities. Clearly, the controller-observer structure must be designed so as to ensure stability of the resulting closed-loop system and adequate tracking performance.

A nonlinear observer for vehicle velocity and acceleration has been proposed in [4], [5], although a combined controller-observer design procedure has not been developed. On the other hand, a passivity-based control law is proposed in [6], where the velocities are reconstructed via a lead filter; however, this control scheme achieves only regulation of position and orientation variables for an underwater vehicle-manipulator system.

In this paper, the problem of output feedback tracking control of subsea vehicle-manipulator systems is addressed. The output

of the controlled system is represented by the position and the attitude of the vehicle, together with the manipulator's joints variables. In order to avoid representation singularities when expressing the vehicle attitude, the unit quaternion is used to express the orientation of the vehicle-fixed frame in lieu of minimal (i.e., three parameters) orientation representations [7].

The new control law proposed here is inspired by the work in [8] in that a model-based control law is designed together with a nonlinear observer for velocity estimation; the two structures are tuned to each other in order to achieve exponential convergence to zero of both motion tracking and estimation errors. It must be noted that, in the control problem considered in this paper, differently from the work in [8], where a simple time-derivative relates position and velocity variables at the joints, a nonlinear mapping exists between orientation variables (unit quaternion) and angular velocity of the vehicle. The presence of this additional nonlinear mapping has been tackled by designing a novel controller-observer structure. Also, a Lyapunov stability analysis has been developed to achieve sufficient conditions on the control and observer parameters ensuring exponential convergence of tracking and estimation errors. It is worth noticing that exponential stability of the closed loop guarantees robustness to unmodeled dynamics and disturbances. Quaternion algebra has been keenly exploited both in the design and in the analysis of the control law.

In view of the limited computational power available in real-time digital control hardware, simplified control laws are suggested, aimed at suitably trading off tracking performance against reduced computational load. Also, the problem of evaluating some dynamic compensation terms, to be properly estimated, is addressed.

A simulation study is carried out based on the data of the experimental vehicle NPS AUV [9]. The same task is executed adopting both the proposed controller-observer scheme and a control law in which velocity is obtained via numerical differentiation of the position measurements. A number of case studies are developed under various operating conditions, i.e., full and partial model knowledge, different quantizer resolutions, and sensor measurements update rates. The results confirm that the chattering on the actuator outputs, due to noise and quantization, is significantly reduced when the controller-observer strategy is adopted, while the tracking performance remains satisfactory even in the presence of poor model knowledge. Hence, better operating conditions for the actuators are achieved without significant degradation of the tracking performance.

II. Modeling

In this section, the mathematical model of a UVMS is presented. The system is modeled as an open kinematic chain composed of a rigid body (the vehicle) and an n-degree-of-freedom rigid-link robot manipulator mounted on the vehicle (see Fig. 1).

A. Kinematics

Let us define an inertial earth-fixed frame $\Sigma_0 = \{O_0, \mathbf{x}_0, \mathbf{y}_0, \mathbf{z}_0\}$ and a vehicle-fixed frame $\Sigma = \{O, \mathbf{x}, \mathbf{y}, \mathbf{z}\}$. The inertial frame is chosen with $\mathbf{z}_0$ parallel to the gravity force vector, $\mathbf{x}_0$ pointing to the north, and $\mathbf{y}_0$ to complete a left-hand frame. The vehicle-fixed frame Σ is usually chosen with $\mathbf{x}$ parallel to the vehicle fore-aft direction, $\mathbf{z}$ parallel to $\mathbf{z}_0$ at vehicle's rest, and $\mathbf{y}$ to complete a left-hand frame.

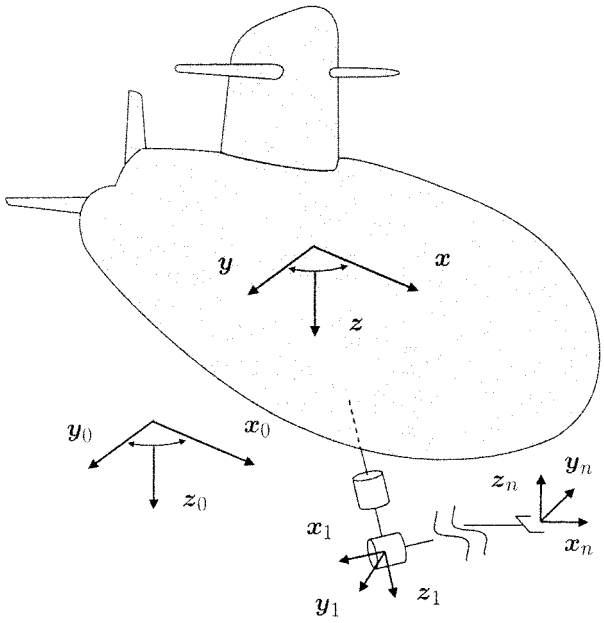

Fig. 1. Sketch of the UVMS with relevant frames.

Hereafter, a superscript will denote the frame to which a vector is referred and will be dropped for brevity whenever a quantity is referred to Σ.

Let $\mathbf{p}^0$ be the (3×1) vector expressing the vehicle position with respect to Σ_0, and $\mathbf{q}$ be the $(n \times 1)$ vector of joint coordinates of the manipulator. The attitude of the vehicle with respect to Σ_0 is expressed by the (3×3) rotation matrix $\mathbf{R}^0$ belonging to the special orthogonal group $SO(3)$ of the rotation matrices [10]. The (6×1) vector of the vehicle's velocity is

$$\boldsymbol{\nu}^0 = \begin{bmatrix} \dot{\mathbf{p}}^0 \\ \boldsymbol{\omega}^0 \end{bmatrix} \tag{1}$$

where $\boldsymbol{\omega}^0$ is the angular velocity of the frame Σ with respect to the frame Σ_0; this satisfies the equality $\dot{\mathbf{R}}^0 = \mathbf{S}(\boldsymbol{\omega}^0)\mathbf{R}^0$, where $\mathbf{S}(\cdot)$ is the skew-symmetric matrix operator performing the cross product.

Finally, the vector of the vehicle's velocity expressed in the frame Σ is

$$\boldsymbol{\nu} = \begin{bmatrix} \mathbf{R}^{0^T}\dot{\mathbf{p}}^0 \\ \mathbf{R}^{0^T}\boldsymbol{\omega}^0 \end{bmatrix} = \begin{bmatrix} \mathbf{v} \\ \boldsymbol{\omega} \end{bmatrix}. \tag{2}$$

B. Dynamics

Assuming that all the bodies in the vehicle-manipulator system are rigid and their masses are constant, the equations of motion can be written in the form

$$\mathbf{M}_R(\mathbf{q})\dot{\boldsymbol{\zeta}} + \mathbf{C}_R(\mathbf{q}, \boldsymbol{\zeta})\boldsymbol{\zeta} = \boldsymbol{\tau} \tag{3}$$

where

$$\boldsymbol{\zeta} = \begin{bmatrix} \boldsymbol{\nu} \\ \dot{\mathbf{q}} \end{bmatrix} \tag{4}$$

is the composite velocity vector of the system. The vector $\boldsymbol{\tau}$ is

$$\boldsymbol{\tau} = \begin{bmatrix} \boldsymbol{\tau}_v \\ \boldsymbol{\tau}_m \end{bmatrix} \tag{5}$$

where $\boldsymbol{\tau}_v$ is the (6×1) vector of forces and moments acting on the vehicle and $\boldsymbol{\tau}_m$ is the $(n \times 1)$ vector of manipulator joint torques. In (3), $\mathbf{M}_R(\mathbf{q})$ is the $(6+n)\times(6+n)$ inertia matrix and $\mathbf{C}_R(\mathbf{q},\boldsymbol{\zeta})\boldsymbol{\zeta}$ is the $(6+n)\times 1$ vector of Coriolis and centrifugal terms.

When the above system of rigid bodies is placed undersea, additional inertia terms must be considered to take into account the effective mass of the surrounding fluid that is accelerated when the bodies move. For a completely submerged system, these additional inertia terms can be collected in a symmetric positive definite matrix $\mathbf{M}_{RA}(\mathbf{q})$, called the added mass matrix [11]–[13]. The corresponding matrix of Coriolis and centrifugal effects $\mathbf{C}_{RA}(\mathbf{q},\boldsymbol{\zeta})$ can always be written as a skew-symmetric matrix. Hence, for the whole system, the mass matrix is given by $\mathbf{M}(\mathbf{q}) = \mathbf{M}_R(\mathbf{q}) + \mathbf{M}_{RA}(\mathbf{q})$, while the matrix of the Coriolis and centrifugal terms is $\mathbf{C}(\mathbf{q},\boldsymbol{\zeta}) = \mathbf{C}_R(\mathbf{q},\boldsymbol{\zeta}) + \mathbf{C}_{RA}(\mathbf{q},\boldsymbol{\zeta})$.

The hydrodynamic damping effects can be taken into account in the equations of motion via the additional term $\mathbf{D}(\mathbf{q},\boldsymbol{\zeta})\boldsymbol{\zeta}$. For a rigid body moving in an irrotational fluid, the matrix $\mathbf{D}$ is nonsymmetric and positive definite; the latter property is due to the dissipative nature of the damping.

It is worth noticing that $\mathbf{M}_{RA}, \mathbf{C}_{RA}$ and $\mathbf{D}$ are to be considered as lumped parameter approximations of the effects due to hydrodynamic forces. More accurate modeling of drag forces and added mass can be achieved by adopting state-dependent coefficients as in [14].

Finally, gravity forces and moments acting on the center of mass and buoyancy forces and moments acting on the center of buoyancy are taken into account via the additional term $\mathbf{g}(\mathbf{q},\mathbf{R}^0)$.

A simplified relationship between the control inputs (provided by joint motors, thrusters, and control surfaces) and the forces and moments acting on the vehicle-manipulator system can be assumed to be of the form [12]

$$\boldsymbol{\tau} = \mathbf{B}\mathbf{u} \tag{6}$$

where $\mathbf{B}$ is a $((6+n)\times p)$ matrix and $\mathbf{u}$ is the $(p \times 1)$ vector of control inputs. In the remainder of this paper, it is assumed that $p \geq (6+n)$ and $\mathbf{B}$ is full-rank. More accurate models of the thruster behavior can be found in [15] and [16].

Therefore, the equations of motion of the UVMS can be written in the form

$$\mathbf{M}(\mathbf{q})\dot{\boldsymbol{\zeta}} + \mathbf{C}(\mathbf{q},\boldsymbol{\zeta})\boldsymbol{\zeta} + \mathbf{D}(\mathbf{q},\boldsymbol{\zeta})\boldsymbol{\zeta} + \mathbf{g}(\mathbf{q},\mathbf{R}^0) = \mathbf{B}\mathbf{u}. \tag{7}$$

It is worth reporting the following useful model properties.

Property 1: The inertia matrix $\mathbf{M}$ of the system is symmetric and positive definite; moreover, it satisfies the inequality $M_m \leq ||\mathbf{M}|| \leq M_M$, where M_m (M_M) is the minimum (maximum) eigenvalue of $\mathbf{M}$.

Property 2: For a suitable choice of the parametrization of $\mathbf{C}$ and if all the single bodies of the system are symmetric, $\dot{\mathbf{M}} - 2\mathbf{C}$ is skew-symmetric [2], which implies $\dot{\mathbf{M}} = \mathbf{C} + \mathbf{C}^T$; moreover, the inequality $||\mathbf{C}(\mathbf{a},\mathbf{b})\mathbf{c}|| \leq C_M||\mathbf{b}||||\mathbf{c}||$ and the equality $\mathbf{C}(\mathbf{a},\alpha_1\mathbf{b}+\alpha_2\mathbf{c}) = \alpha_1\mathbf{C}(\mathbf{a},\mathbf{b}) + \alpha_2\mathbf{C}(\mathbf{a},\mathbf{c})$ hold.

Property 3: The matrix $\mathbf{D}$ is positive definite and satisfies $||\mathbf{D}(\mathbf{q},\mathbf{a}) - \mathbf{D}(\mathbf{q},\mathbf{b})|| \leq D_M||\mathbf{a}-\mathbf{b}||$.

III. Attitude Representation

Throughout the paper, a quaternion-based description of the vehicle attitude is used (see [17]). In fact, the use of the unit quaternion in lieu of a minimal representation of the orientation (e.g., Euler angles) allows one to overcome the problems arising from representation singularities; also, the unit quaternion possesses nice computational properties [18]. A few basic concepts regarding unit quaternions are summarized here.

The orientation of a given frame Σ_a with respect to a reference frame can be expressed via a four-parameter representation in terms of the unit quaternion (viz. Euler parameters)

$$\mathcal{Q}_a = \{\eta_a, \epsilon_a\} = \left\{\cos\frac{\theta}{2}, \mathbf{k}\sin\frac{\theta}{2}\right\} \tag{8}$$

where θ and $\mathbf{k}$, respectively, are the rotation angle and the (3×1) unit vector of an equivalent angle/axis description of the orientation. Notice that the scalar part η_a and the vector part ϵ_a are constrained on the unit radius sphere of $\mathbb{R}^4$, i.e.,

$$\eta_a^2 + \epsilon_a^T\epsilon_a = 1. \tag{9}$$

Moreover, $\mathcal{Q}_a = \{\eta_a, \epsilon_a\}$ and $\mathcal{Q}'_a = \{-\eta_a, -\epsilon_a\}$ represent the same orientation, and frame Σ_a is aligned to the reference frame as long as $\eta_a = \pm 1$ and $\epsilon_a = \mathbf{0}$.

The mutual orientation between the frames Σ_a and Σ_b can be described by the rotation matrix $\mathbf{R}_b^a = \mathbf{R}_a^T\mathbf{R}_b$. The corresponding unit quaternion can be either extracted directly from $\mathbf{R}_b^a$ [19] or computed by the composition (quaternion product) of the unit quaternions $\mathcal{Q}_a^{-1} = \{\eta_a, -\epsilon_a\}$ and $\mathcal{Q}_b = \{\eta_b, \epsilon_b\}$

$$\tilde{\mathcal{Q}}_{ba} = \{\tilde{\eta}_{ba}, \tilde{\epsilon}_{ba}^a\} = \mathcal{Q}_a^{-1} * \mathcal{Q}_b \tag{10}$$

where * denotes the quaternion product defined as

$$\mathcal{Q}_a * \mathcal{Q}_b = \left\{\eta_a\eta_b - \epsilon_a^T\epsilon_b, \eta_a\epsilon_b + \eta_b\epsilon_a + \mathbf{S}(\epsilon_a)\epsilon_b\right\}. \tag{11}$$

If the two frames are aligned, it is $\mathbf{R}_b^a = \mathbf{I}_3$, where $\mathbf{I}_l$ denotes the $(l \times l)$ identity matrix. In this case, $\tilde{\eta}_{ba} = \pm 1$ and $\tilde{\epsilon}_{ba}^a = \mathbf{0}$ and, thus, the sole vector part can be used to represent an orientation error. Notice that $\tilde{\epsilon}_{ba}^a = \tilde{\epsilon}_{ba}^b$, i.e., the quaternion components can be indifferently expressed in either of the two frames.

The relationship between the time derivative of the quaternion components and the angular velocity $\tilde{\boldsymbol{\omega}}_{ba}^a = \mathbf{R}_a^T(\boldsymbol{\omega}_b - \boldsymbol{\omega}_a)$ of the frame Σ_b relative to the frame Σ_a, expressed in the frame Σ_a, is established by the so-called quaternion propagation rule

$$\dot{\tilde{\eta}}_{ba} = -\frac{1}{2}\tilde{\epsilon}_{ba}^{aT}\tilde{\boldsymbol{\omega}}_{ba}^a \tag{12}$$

$$\dot{\tilde{\epsilon}}_{ba}^a = \frac{1}{2}\mathbf{E}(\tilde{\mathcal{Q}}_{ba})\tilde{\boldsymbol{\omega}}_{ba}^a \tag{13}$$

where

$$\mathbf{E}(\tilde{\mathcal{Q}}_{ba}) = \tilde{\eta}_{ba}\mathbf{I}_3 - \mathbf{S}\left(\tilde{\epsilon}_{ba}^a\right). \tag{14}$$

In the following, the vehicle attitude with respect to the earth-fixed frame will be represented by the unit quaternion $\mathcal{Q} = \{\eta, \epsilon\}$ corresponding to the rotation matrix $\mathbf{R}^0$.

IV. Generation of the Desired Trajectories

The desired position for the vehicle is assigned in terms of the vector $\mathbf{p}_d^0(t)$, while the commanded attitude trajectory can be assigned in terms of the rotation matrix $\mathbf{R}_d^0(t)$ expressing the orientation of the desired vehicle frame Σ_d with respect to Σ_0. Equivalently, the desired orientation can be expressed in terms of the unit quaternion $\mathcal{Q}_d(t)$ corresponding to $\mathbf{R}_d^0(t)$. Finally, the desired joint motion is assigned in terms of the vector of joint variables $\mathbf{q}_d(t)$. Notice that, if the desired trajectory is assigned in terms of task variables, the quantities above can be obtained by a kinematic control approach [20].

The desired velocity vectors are denoted by $\dot{\mathbf{p}}_d^0(t)$, $\boldsymbol{\omega}_d^0(t)$, and $\dot{\mathbf{q}}_d(t)$, while the desired accelerations are assigned in terms of the vectors $\ddot{\mathbf{p}}_d^0(t)$, $\dot{\boldsymbol{\omega}}_d^0(t)$, and $\ddot{\mathbf{q}}_d(t)$.

Notice that all the desired quantities are naturally assigned with respect to the earth-fixed frame Σ_0; the corresponding position and velocity in the vehicle-fixed frame Σ are computed as

$$\mathbf{p}_d = \mathbf{R}^{0T}\mathbf{p}_d^0, \quad \boldsymbol{\zeta}_d = \begin{bmatrix} \mathbf{R}^{0T}\dot{\mathbf{p}}_d^0 \\ \mathbf{R}^{0T}\boldsymbol{\omega}_d^0 \\ \dot{\mathbf{q}}_d \end{bmatrix} = \begin{bmatrix} \mathbf{v}_d \\ \boldsymbol{\omega}_d \\ \dot{\mathbf{q}}_d \end{bmatrix}. \tag{15}$$

It is worth pointing out that the computation of the desired acceleration $\dot{\boldsymbol{\zeta}}_d$ requires knowledge of the actual angular velocity $\boldsymbol{\omega}$; in fact, in view of $\dot{\mathbf{R}}^{0T} = -\mathbf{S}(\boldsymbol{\omega})\mathbf{R}^{0T}$, it is

$$\dot{\boldsymbol{\zeta}}_d = \begin{bmatrix} \mathbf{R}^{0T}\ddot{\mathbf{p}}_d^0 - \mathbf{S}(\boldsymbol{\omega})\mathbf{v}_d \\ \mathbf{R}^{0T}\dot{\boldsymbol{\omega}}_d^0 - \mathbf{S}(\omega)\boldsymbol{\omega}_d \\ \ddot{\mathbf{q}}_d \end{bmatrix}. \tag{16}$$

Hence, it is convenient to use in the control law the modified acceleration vector defined as

$$\mathbf{a}_d = \begin{bmatrix} \mathbf{R}^{0T}\ddot{\mathbf{p}}_d^0 - \mathbf{S}(\boldsymbol{\omega}_d)\mathbf{v}_d \\ \mathbf{R}^{0T}\dot{\boldsymbol{\omega}}_d^0 - \mathbf{S}(\boldsymbol{\omega}_d)\boldsymbol{\omega}_d \\ \ddot{\mathbf{q}}_d \end{bmatrix} \tag{17}$$

which can be evaluated without using the actual velocity; the two vectors are related by the equality

$$\dot{\boldsymbol{\zeta}}_d = \mathbf{a}_d + \mathbf{S}_{PO}(\tilde{\boldsymbol{\omega}}_d)\boldsymbol{\zeta}_d \tag{18}$$

where $\mathbf{S}_{PO}(\cdot) = \mathrm{diag}\{\mathbf{S}(\cdot), \mathbf{S}(\cdot), \mathbf{O}_n\}$, $\mathbf{O}_l$ denotes the $(l \times l)$ null matrix, and $\tilde{\boldsymbol{\omega}}_d = \boldsymbol{\omega}_d - \boldsymbol{\omega}$.

Hereafter, it is assumed that $\|\boldsymbol{\zeta}_d(t)\| \leq \zeta_{dM}$ for all $t \geq 0$.

V. Control Law

Consider a UVMS performing a manipulation task where accurate trajectory tracking for the manipulator's end effector is required, while the vehicle is to be kept in a hovering mode. In order to accomplish the task, accurate position and orientation measurements are required at a relatively high update rate: this can be achieved, e.g., if the system is equipped with a vision-based sensing device. Moreover, the availability of accurate and noise-free velocity measurements is crucial for achieving good tracking performance; unfortunately, this is usually not guaranteed by Doppler effect sensors and sonars, especially at low velocities. As a matter of fact, the use of numerical differentiation of noisy position/orientation measurements may lead to chattering of the control inputs and, thus, to high-energy consumption and a reduced lifetime of the actuators.

It is worth noticing that low-pass filtering of the numerically reconstructed velocities may significantly degrade the system's dynamic behavior and, eventually, affect the closed-loop stability. In other words, such a filter has to be designed together with the controller so as to preserve closed-loop stability and good tracking performance.

This is the basic idea which inspired the approach described in the following: namely, a nonlinear filter (observer) on the position and attitude measures is designed, together with a model-based controller so as to achieve exponential stability and ensure tracking of the desired position and attitude trajectories.

A tracking control law is naturally based on the *tracking error*

$$\mathbf{e}_d = \begin{bmatrix} \tilde{\mathbf{p}}_d \\ \tilde{\epsilon}_d \\ \tilde{\mathbf{q}}_d \end{bmatrix} \tag{19}$$

where $\tilde{\mathbf{p}}_d = \mathbf{p}_d - \mathbf{p}$, $\tilde{\mathbf{q}}_d = \mathbf{q}_d - \mathbf{q}$ and $\tilde{\epsilon}_d$ is the vector part of the unit quaternion $\tilde{\mathcal{Q}}_d = \mathcal{Q}^{-1} * \mathcal{Q}_d$.

It must be noticed that a derivative control action based on (19) would require velocity measurements in the control loop. In the absence of velocity measurements, a suitable estimate $\boldsymbol{\zeta}_e$ of the velocity vector has to be considered. Let also $\mathbf{p}_e$ and $\mathcal{Q}_e$ denote the estimated position and attitude of the vehicle, respectively; the estimated joint variables are denoted by $\mathbf{q}_e$. Hence, the following error vector has to be considered:

$$\mathbf{e}_{de} = \begin{bmatrix} \tilde{\mathbf{p}}_{de} \\ \tilde{\epsilon}_{de}^e \\ \tilde{\mathbf{q}}_{de} \end{bmatrix} \tag{20}$$

where $\tilde{\mathbf{p}}_{de} = \mathbf{p}_d - \mathbf{p}_e$, $\tilde{\mathbf{q}}_{de} = \mathbf{q}_d - \mathbf{q}_e$, and $\tilde{\epsilon}_{de}^e$ is the vector part of the unit quaternion

$$\tilde{\mathcal{Q}}_{de} = \mathcal{Q}_e^{-1} * \mathcal{Q}_d.$$

In order to avoid direct velocity feedback, the corresponding velocity error can be defined as

$$\tilde{\boldsymbol{\zeta}}_{de} = \begin{bmatrix} \mathbf{R}^{0T}\dot{\tilde{\mathbf{p}}}_{de}^0 - \mathbf{S}(\boldsymbol{\omega}_d)\tilde{\mathbf{p}}_{de} \\ \dot{\tilde{\epsilon}}_{de}^e \\ \dot{\tilde{\mathbf{q}}}_{de} \end{bmatrix} \tag{21}$$

which is related to the time derivative of $\mathbf{e}_{de}$ as follows:

$$\dot{\mathbf{e}}_{de} = \tilde{\boldsymbol{\zeta}}_{de} + \mathbf{S}_P(\tilde{\boldsymbol{\omega}}_d)\mathbf{e}_{de} \tag{22}$$

where $\mathbf{S}_P(\cdot) = \mathrm{diag}\{\mathbf{S}(\cdot), \mathbf{O}_3, \mathbf{O}_n\}$.

In order to design an observer providing velocity estimates, the *estimation error* has to be considered

$$\mathbf{e}_e = \begin{bmatrix} \tilde{\mathbf{p}}_e \\ \tilde{\epsilon}_e \\ \tilde{\mathbf{q}}_e \end{bmatrix} \tag{23}$$

where $\tilde{\mathbf{p}}_e = \mathbf{p}_e - \mathbf{p}$, $\tilde{\mathbf{q}}_e = \mathbf{q}_e - \mathbf{q}$, and $\tilde{\epsilon}_e$ is the vector part of the unit quaternion $\tilde{\mathcal{Q}}_e = \mathcal{Q}^{-1} * \mathcal{Q}_e$.

Finally, consider the vectors

$$\boldsymbol{\zeta}_r = \boldsymbol{\zeta}_d + \boldsymbol{\Lambda}_d\mathbf{e}_{de} \tag{24}$$

$$\boldsymbol{\zeta}_o = \boldsymbol{\zeta}_e + \boldsymbol{\Lambda}_e\mathbf{e}_e. \tag{25}$$

where $\boldsymbol{\Lambda}_d = \mathrm{diag}\{\boldsymbol{\Lambda}_{dP}, \lambda_{dO}\mathbf{I}_3, \boldsymbol{\Lambda}_{dQ}\}$ and $\boldsymbol{\Lambda}_e = \mathrm{diag}\{\boldsymbol{\Lambda}_{eP}, \lambda_{eO}\mathbf{I}_3, \boldsymbol{\Lambda}_{eQ}\}$ are diagonal and positive definite matrices. It is

worth remarking that $\boldsymbol{\zeta}_r$ and $\boldsymbol{\zeta}_o$ can be evaluated without using the actual velocity $\boldsymbol{\zeta}$.

The proposed control law is

$$\mathbf{u} = \mathbf{B}^{\dagger}\left(\mathbf{M}(\mathbf{q})\mathbf{a}_r + \mathbf{C}(\mathbf{q},\boldsymbol{\zeta}_o)\boldsymbol{\zeta}_r + \mathbf{K}_v(\boldsymbol{\zeta}_r - \boldsymbol{\zeta}_o) + \mathbf{K}_p\mathbf{e}_d + \mathbf{g}(\mathbf{q},\mathbf{R}^0) + \frac{1}{2}\mathbf{D}(\mathbf{q},\boldsymbol{\zeta}_r)(\boldsymbol{\zeta}_r + \boldsymbol{\zeta}_o)\right) \tag{26}$$

where $\mathbf{K}_p = \mathrm{diag}\{k_{pP}\mathbf{I}_3, k_{pO}\mathbf{I}_3, \mathbf{K}_{pQ}\}$ is a diagonal positive definite matrix and $\mathbf{K}_v$ is a symmetric positive definite matrix. The reference acceleration vector $\mathbf{a}_r$ is defined as

$$\mathbf{a}_r = \mathbf{a}_d + \boldsymbol{\Lambda}_d\tilde{\zeta}_{de} \tag{27}$$

and thus the control law (26) does not require feedback of the vehicle and/or manipulator velocities.

The estimated velocity vector $\boldsymbol{\zeta}_e$ is obtained via the observer defined by (28), shown at the bottom of the page, where the matrix $\mathbf{L}_p = \mathrm{diag}\{l_{pP}\mathbf{I}_3, l_{pO}\mathbf{I}_3, \mathbf{L}_{pQ}\}$ is diagonal positive definite. The matrix $\mathbf{L}_v = \mathrm{diag}\{\mathbf{L}_{vP}, l_{vO}\mathbf{I}_3, \mathbf{L}_{vQ}\}$ is symmetric and positive definite, and

$$\mathbf{A}(\tilde{\mathcal{Q}}_e) = \mathrm{diag}\{\mathbf{I}_3,\ \mathbf{E}(\tilde{\mathcal{Q}}_e)/2,\ \mathbf{I}_n\}. \tag{29}$$

The estimated quantities $\mathbf{p}_e^0$ and $\mathbf{q}_e$ are computed by integrating the corresponding estimated velocities $\dot{\mathbf{p}}_e^0 = \mathbf{R}^0\mathbf{v}_e$ and $\dot{\mathbf{q}}_e$, respectively, whereas the estimated orientation $\mathcal{Q}_e$ is computed from the estimated angular velocity $\boldsymbol{\omega}_e^0 = \mathbf{R}^0\boldsymbol{\omega}_e$ via the quaternion propagation rule.

In order to derive the closed-loop dynamic equations, it is useful to define the variables

$$\boldsymbol{\sigma}_d = \boldsymbol{\zeta}_r - \boldsymbol{\zeta} = \tilde{\boldsymbol{\zeta}}_d + \boldsymbol{\Lambda}_d\mathbf{e}_{de} \tag{30}$$

$$\boldsymbol{\sigma}_e = \boldsymbol{\zeta}_o - \boldsymbol{\zeta} = \tilde{\boldsymbol{\zeta}}_e + \boldsymbol{\Lambda}_e\mathbf{e}_e \tag{31}$$

where

$$\tilde{\boldsymbol{\zeta}}_d = \boldsymbol{\zeta}_d - \boldsymbol{\zeta} \tag{32}$$

$$\tilde{\boldsymbol{\zeta}}_e = \boldsymbol{\zeta}_e - \boldsymbol{\zeta}. \tag{33}$$

Combining (7) with the control law (26), (27), and using the equality

$$\mathbf{a}_r = \dot{\boldsymbol{\zeta}}_r + \mathbf{S}_{PO}(\tilde{\boldsymbol{\omega}}_d)\boldsymbol{\zeta}_d + \boldsymbol{\Lambda}_d\mathbf{S}_P(\tilde{\boldsymbol{\omega}}_d)\mathbf{e}_{de} \tag{34}$$

the tracking error dynamics can be derived as

$$\begin{aligned}\mathbf{M}(\mathbf{q})\dot{\boldsymbol{\sigma}}_d + \mathbf{C}(\mathbf{q},\boldsymbol{\zeta})\boldsymbol{\sigma}_d + \mathbf{K}_v\boldsymbol{\sigma}_d - \mathbf{K}_p\mathbf{e}_d &= \mathbf{K}_v\boldsymbol{\sigma}_e - \mathbf{C}(\mathbf{q},\boldsymbol{\sigma}_e)\boldsymbol{\zeta}_r - \mathbf{M}(\mathbf{q})\mathbf{S}_{PO}(\tilde{\boldsymbol{\omega}}_d)\boldsymbol{\zeta}_d \\ &\quad - \mathbf{M}(\mathbf{q})\boldsymbol{\Lambda}_d\mathbf{S}_P(\tilde{\boldsymbol{\omega}}_d)\mathbf{e}_{de} + \mathbf{D}(\mathbf{q},\boldsymbol{\zeta})\boldsymbol{\zeta} \\ &\quad - \frac{1}{2}\mathbf{D}(\mathbf{q},\boldsymbol{\zeta}_r)(\boldsymbol{\zeta}_r + \boldsymbol{\zeta}_o).\end{aligned} \tag{35}$$

TABLE I
COMPUTATIONAL BURDEN

	mult/div	add/sub
Control law (26),(28)	1831	1220
Control law (38),(39)	1216	849
Control law (40),(41)	354	147

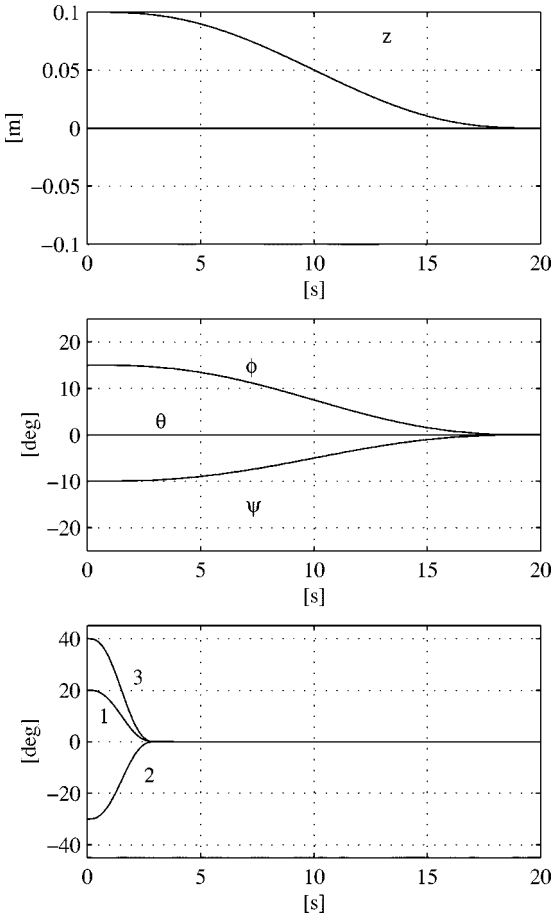

Fig. 2. Desired trajectories used in all the case studies. Top: vehicle position. Middle: vehicle orientation (RPY angles). Bottom: joint positions.

The observer equation (28) together with (35) yields the estimation error dynamics

$$\begin{aligned}\mathbf{M}(\mathbf{q})\dot{\boldsymbol{\sigma}}_e + (\mathbf{L}_v\mathbf{A}(\tilde{\mathcal{Q}}_e) - \mathbf{K}_v)\boldsymbol{\sigma}_e - \mathbf{L}_p\mathbf{e}_e &= -\mathbf{K}_v\boldsymbol{\sigma}_d - \mathbf{C}(\mathbf{q},\boldsymbol{\zeta})\boldsymbol{\sigma}_e + \mathbf{C}^T(\mathbf{q},\boldsymbol{\sigma}_d)\boldsymbol{\zeta}_o + \mathbf{D}(\mathbf{q},\boldsymbol{\zeta})\boldsymbol{\zeta} \\ &\quad - \frac{1}{2}\mathbf{D}(\mathbf{q},\boldsymbol{\zeta}_r)(\boldsymbol{\zeta}_r + \boldsymbol{\zeta}_o).\end{aligned} \tag{36}$$

A state vector for the closed-loop system (35) and (36) is then

$$\mathbf{x} = \begin{bmatrix}\boldsymbol{\sigma}_d \\ \mathbf{e}_d \\ \boldsymbol{\sigma}_e \\ \mathbf{e}_e\end{bmatrix}. \tag{37}$$

$$\begin{cases}\dot{\mathbf{z}} = \mathbf{M}(\mathbf{q})\mathbf{a}_r - (\mathbf{L}_p + \mathbf{L}_v\mathbf{A}(\tilde{\mathcal{Q}}_e)\boldsymbol{\Lambda}_e)\mathbf{e}_e + \mathbf{K}_p\mathbf{e}_d + \mathbf{C}(\mathbf{q},\boldsymbol{\zeta}_o)\boldsymbol{\zeta}_r + \mathbf{C}^T(\mathbf{q},\boldsymbol{\zeta}_r)\boldsymbol{\zeta}_o \\ \boldsymbol{\zeta}_e = \mathbf{M}^{-1}(\mathbf{q})(\mathbf{z} - \mathbf{L}_v\mathbf{e}_e) - \boldsymbol{\Lambda}_e\mathbf{e}_e,\end{cases} \tag{28}$$

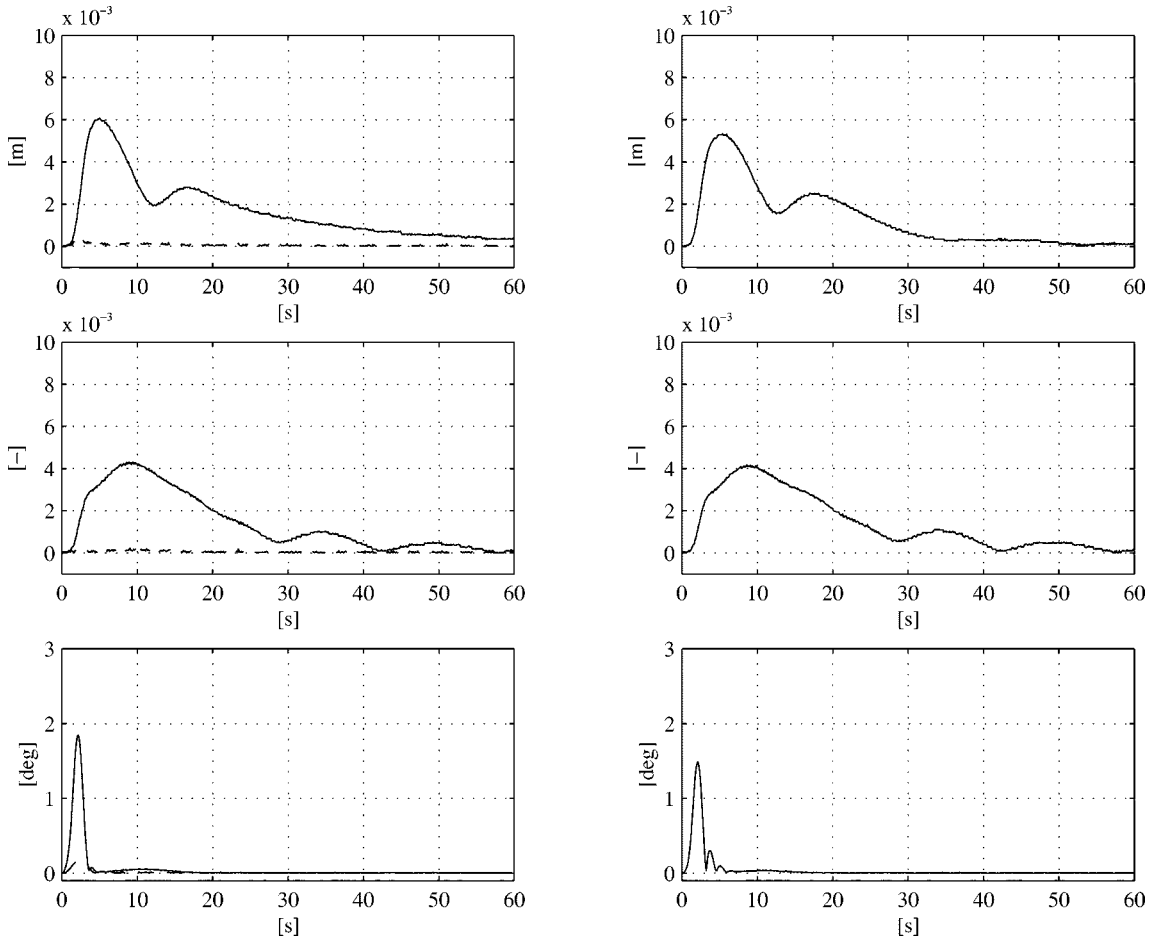

Fig. 3. Comparison of the control laws (38), (39), and (43): norm of the tracking (solid line) and estimation (dashed line) errors. Left: control laws (38) and (39). Right: control law (43). Top: vehicle position error. Middle: vehicle orientation error (vector part of the quaternion). Bottom: joint position errors. Both controllers guarantee good performance in terms of tracking errors.

Notice that perfect tracking of the desired motion together with the exact estimate of the system velocities results in $\mathbf{x} = \mathbf{0}$. Therefore, the control objective is fulfilled iff the closed loop system (35) and (36) is asymptotically stable at the origin of its state space. This is ensured by the following theorem (whose proof is in the Appendix):

Theorem: There exists a choice of the controller gains $\mathbf{K}_p, \mathbf{K}_v, \mathbf{\Lambda}_d$ and of the observer parameters $\mathbf{L}_p, \mathbf{L}_v, \mathbf{\Lambda}_e$ such that the origin of the state space of system (35) and (36) is locally exponentially stable.

VI. Implementation Issues

Implementation of the controller-observer scheme (26) and (28) requires computation of the dynamic compensation terms. While this can be done quite effectively for the terms related to rigid body dynamics, the terms related to hydrodynamic effects are usually affected by some degree of approximation and/or uncertainty. Besides the use of adaptive control schemes aimed at online estimation of relevant model parameters, e.g., [13], [21], [22], it is important to have an estimate of the main hydrodynamic coefficients.

An estimate of the added mass coefficients can be obtained via strip theory [12].

A rough approximation of the hydrodynamic damping is obtained by considering only the linear skin friction and the drag-generalized forces. The drag is usually assumed to be proportional to the square of the relative velocity of the rigid body with respect to the fluid, while the skin friction is assumed to be proportional to the relative velocity. Of course, this may not be a good approximation of hydrodynamic damping for some cases (e.g., the power of the relative velocity may be not unitary for particular geometries). More accurate estimates can be obtained by taking into account the geometry of the body [1] or via experimental identification [9].

Another important point concerns the computational complexity associated with dynamic compensation against the limited computing power typically available on-board. This might suggest the adoption of a control law computationally lighter than the one derived above. A reasonable compromise between tracking performance and computational burden is achieved if the compensation of Coriolis, centripetal and damping terms are omitted, resulting in the controller

$$\mathbf{u} = \mathbf{B}^{\dagger}(\mathbf{M}(\mathbf{q})\mathbf{a}_r + \mathbf{K}_v(\boldsymbol{\zeta}_r - \boldsymbol{\zeta}_o) + \mathbf{K}_p\mathbf{e}_d + \mathbf{g}(\mathbf{q}, \mathbf{R}^0)) \quad (38)$$

with the simplified observer

$$\begin{cases} \dot{\mathbf{z}} = \mathbf{M}(\mathbf{q})\mathbf{a}_r - (\mathbf{L}_p + \mathbf{L}_v\mathbf{A}(\tilde{\mathcal{Q}}_e)\mathbf{\Lambda}_e)\mathbf{e}_e + \mathbf{K}_p\mathbf{e}_d \\ \boldsymbol{\zeta} = \mathbf{M}^{-1}(\mathbf{q})(\mathbf{z} - \mathbf{L}_v\mathbf{e}_e) - \mathbf{\Lambda}_e\mathbf{e}_e, \end{cases} \quad (39)$$

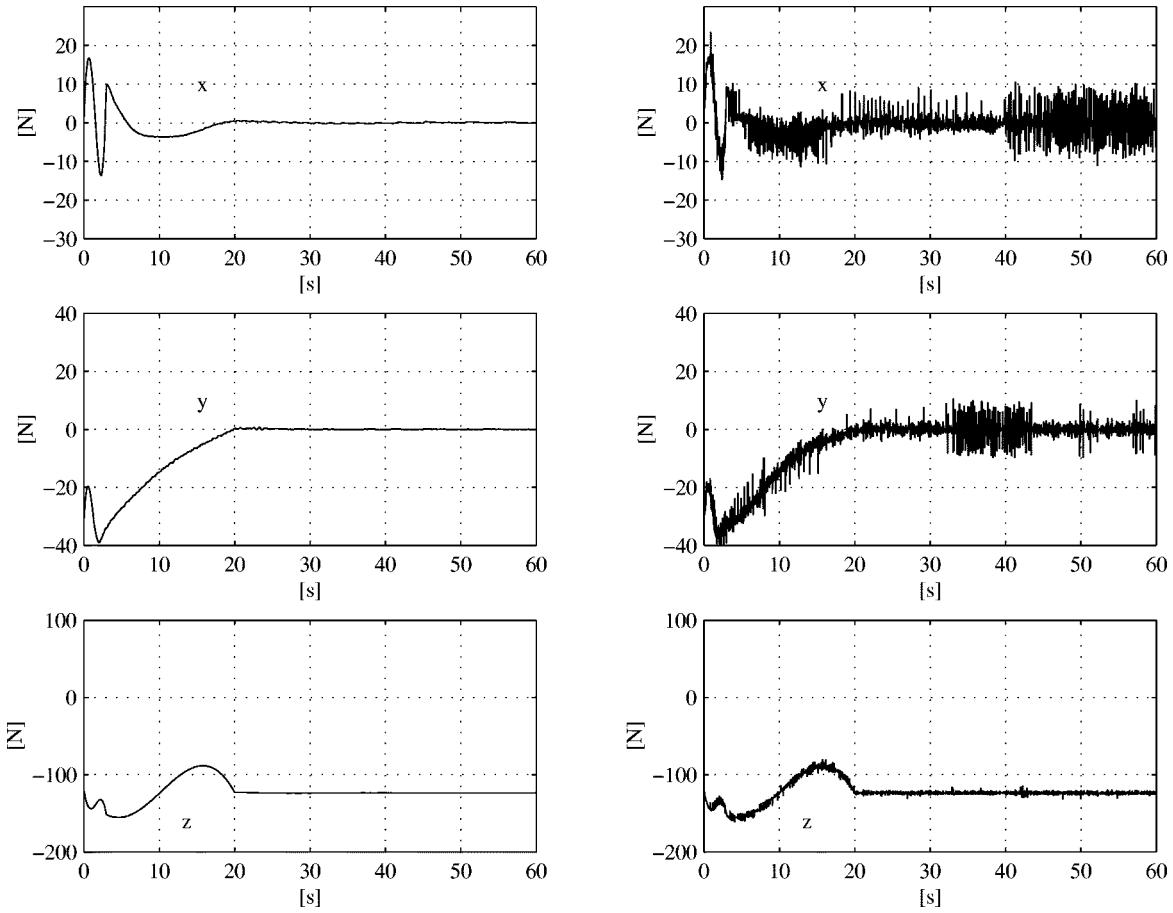

Fig. 4. Comparison of the control laws (38), (39), and (43): vehicle control forces. Left: control laws (38) and (39). Right: control law (43). The proposed controller-observer scheme avoids the chattering that arises with the law (43).

The computational load can be further reduced if a suitable constant diagonal inertia matrix $\hat{\mathbf{M}}$ is used in lieu of the matrix $\mathbf{M}(\mathbf{q})$, i.e.,

$$\mathbf{u} = \mathbf{B}^{\dagger}(\hat{\mathbf{M}}\mathbf{a}_r + \mathbf{K}_v(\boldsymbol{\zeta}_r - \boldsymbol{\zeta}_o) + \mathbf{K}_p\mathbf{e}_d + \mathbf{g}(\mathbf{q}, \mathbf{R}^0)) \quad (40)$$

with the observer

$$\begin{cases} \dot{\mathbf{z}} = \hat{\mathbf{M}}\mathbf{a}_r - (\mathbf{L}_p + \mathbf{L}_v\mathbf{A}(\tilde{\mathcal{Q}}_e)\boldsymbol{\Lambda}_e)\mathbf{e}_e + \mathbf{K}_p\mathbf{e}_d \\ \hat{\boldsymbol{\zeta}} = \hat{\mathbf{M}}^{-1}(\mathbf{z} - \mathbf{L}_v\mathbf{e}_e) - \boldsymbol{\Lambda}_e\mathbf{e}_e, \end{cases} \quad (41)$$

Table I shows the computational load of each control law, in terms of required floating point operations, in the case of a six-degree-of-freedom vehicle equipped with a three-degree-of-freedom manipulator. Where required, inversion of the inertia matrix has been obtained via the Cholesky factorization since $\mathbf{M}(\mathbf{q})$ is symmetric and positive definite; of course, the inverse of the constant matrix $\hat{\mathbf{M}}$ is computed once off-line. As shown by the results in Table I, the computational load is reduced by about 80% when the control law (40), (41) is considered.

It is understood that approximate compensation of the system dynamics results in reduced tracking/estimation performance of the control system, which depends on the magnitude of the uncertainty. It must be pointed out that exponential stability of the closed-loop system ensures robustness to uncertainties and disturbances. However, a rigorous robustness analysis would become cumbersome and may lead to a set of too conservative bounds.

VII. Simulation Results

Numerical simulations have been performed in order to show the effectiveness of the proposed control law. The UVMS simulator, developed using MATLAB 4.2 with a SIMULINK 1.3 environment, is described in [23]. Modularity of the software allows the user to define the number of links and the structure of the manipulator arm as well as to change system and environmental parameters.

The vehicle data are taken from [9]; they refer to the experimental autonomous underwater vehicle NPS AUV Phoenix. In this paper, a three-link manipulator with an elbow kinematic structure mounted under the vehicle body has been considered. The dry weight of the vehicle is $\approx$5000 kg, while the dry weight of the manipulator is $\approx$170 kg. The length of the vehicle is 5.5 m, while the length of each link is $\approx$1 m; the center of gravity is coincident with the center of buoyancy and it is supposed to be in the geometrical center of the body. Because the vehicle is neutrally buoyant, but the arm is not, the whole system is not neutrally buoyant. Links are cylindrical, thus hydrodynamic effects can be computed by simplified relations as in [1]. Dry and viscous joint friction is also taken into account. Matrix $\mathbf{B}$ is assumed to be constant and full-rank

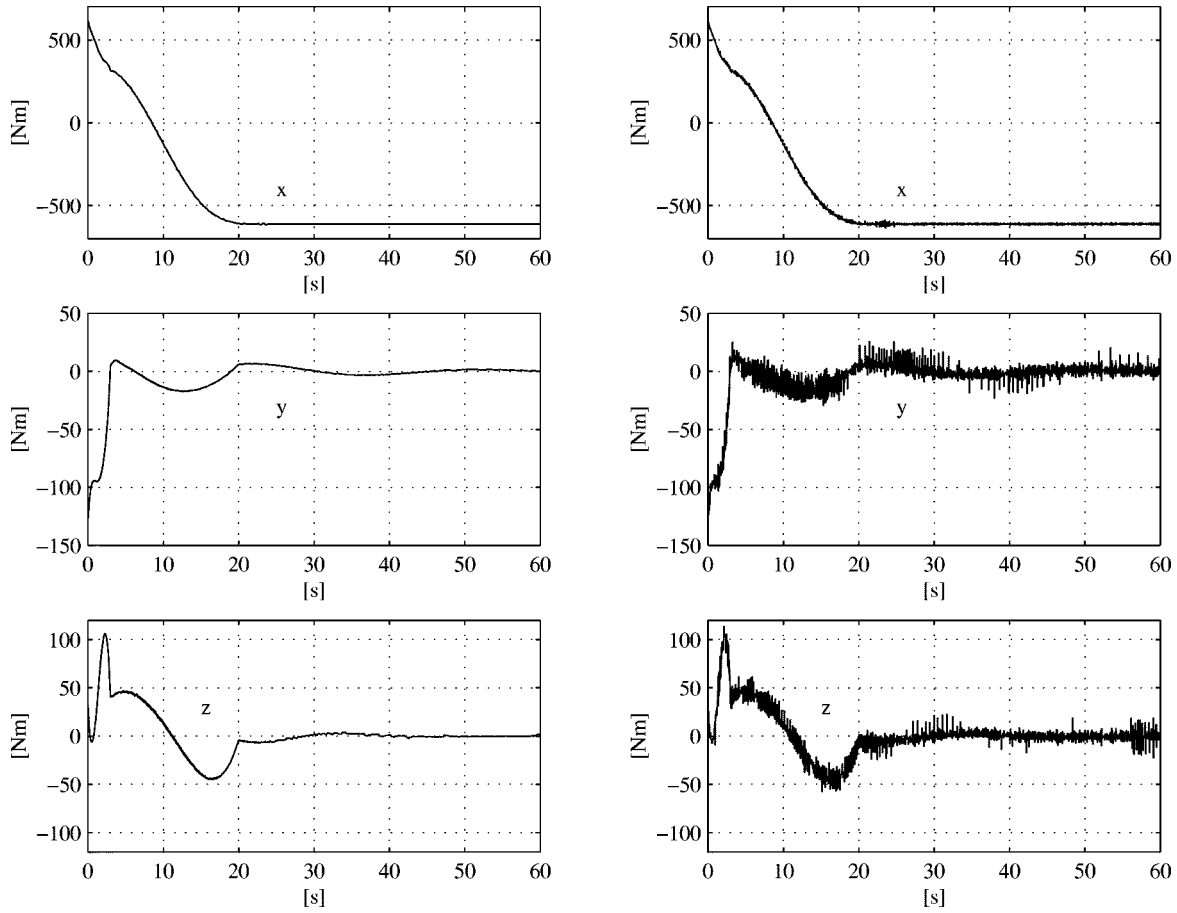

Fig. 5. Comparison of the control laws (38), (39), and (43): vehicle control moments. Left: control laws (38) and (39); Right: control law (43). Notice that, due to the final configuration of the manipulator and the vehicle's centers of gravity/buoyancy, the moment about $\mathbf{x}$ is the only non-null value at steady state.

(for simplicity, it has been set to identity), meaning that direct control of the forces and moments acting on the vehicle and joint torques is available.

A task involving motion of both the vehicle and the manipulator has been considered. At the initial time, the vehicle is at the location $\boldsymbol{\eta}_i = [0\,0\,0.1\,15\,0\,-15]^T$ [m, deg] and the manipulator is at $\mathbf{q}_i = [20\,-30\,40]^T$ [deg]. The vehicle must move to the final location $\boldsymbol{\eta}_f = [0\,0\,0\,0\,0\,0]^T$ [m, deg] in 20 s according to a fifth-order polynomial time law. The manipulator must move to $\mathbf{q}_f = [0\,0\,0]^T$ [deg] in 3 s according to a fifth-order polynomial time law. Notice that the assigned trajectories correspond to a fast desired motion for the manipulator while the vehicle is kept almost hovering. Fig. 2 shows the desired trajectories. It must be noticed that the vehicle orientation set point is assigned in terms of Euler angles, as is typical in navigation planning; these are converted into the corresponding rotation matrix so as to extract the quaternion expressing the orientation error. Remarkably, this procedure is free of singularities [19].

A. First Case Study

The performance of the control laws (38) and (39) has been compared to that obtained with a control scheme of similar structure in which the velocity feedback is implemented through the numerical differentiation of position measurements. The following control law was then considered:

$$\mathbf{u} = \mathbf{B}^{\dagger}(\mathbf{M}(\mathbf{q})\dot{\boldsymbol{\zeta}}_r + \mathbf{C}(\mathbf{q},\boldsymbol{\zeta})\boldsymbol{\zeta}_r + \mathbf{K}_v(\boldsymbol{\zeta}_r - \boldsymbol{\zeta}) + \mathbf{K}_p\mathbf{e}_d + \mathbf{g}(\mathbf{q},\mathbf{R}^0)) \tag{42}$$

where $\boldsymbol{\zeta}_r = \boldsymbol{\zeta}_d + \boldsymbol{\Lambda}_d\mathbf{e}_d$. $\boldsymbol{\zeta}$ and $\dot{\boldsymbol{\zeta}}_r$ are computed via the first-order difference. The above control law is analogous to the operational space control law proposed in [24] and extended in [25] in the framework of quaternion-based attitude control. To obtain a control law of computational complexity similar to that of (38), the algorithm (42) has been modified into the simpler form

$$\mathbf{u} = \mathbf{B}^{\dagger}(\mathbf{M}(\mathbf{q})\dot{\boldsymbol{\zeta}}_r + \mathbf{K}_v(\boldsymbol{\zeta}_r - \boldsymbol{\zeta}) + \mathbf{K}_p\mathbf{e}_d + \mathbf{g}(\mathbf{q},\mathbf{R}^0)). \tag{43}$$

The parameters in the control laws are set to

$$\begin{aligned}
\boldsymbol{\Lambda}_d &= \mathrm{diag}\{0.005\mathbf{I}_3, 0.01\mathbf{I}_3, 0.01\mathbf{I}_3\}\\
\boldsymbol{\Lambda}_e &= \mathrm{diag}\{5\mathbf{I}_3, 10\mathbf{I}_3, 10, 10, 5\}\\
\mathbf{L}_v &= \mathrm{diag}\{1\mathbf{I}_3, 20\mathbf{I}_3, 160, 160, 900\}\\
\mathbf{L}_p &= \mathrm{diag}\{5000\mathbf{I}_3, 10^5\mathbf{I}_3, 10^3, 10^3, 2\cdot 10^3\}\\
\mathbf{K}_p &= \mathrm{diag}\{400\mathbf{I}_3, 500\mathbf{I}_3, 1500\mathbf{I}_3\}\\
\mathbf{K}_v &= \mathrm{diag}\{4000\mathbf{I}_3, 4000\mathbf{I}_3, 400\mathbf{I}_3\}.
\end{aligned}$$

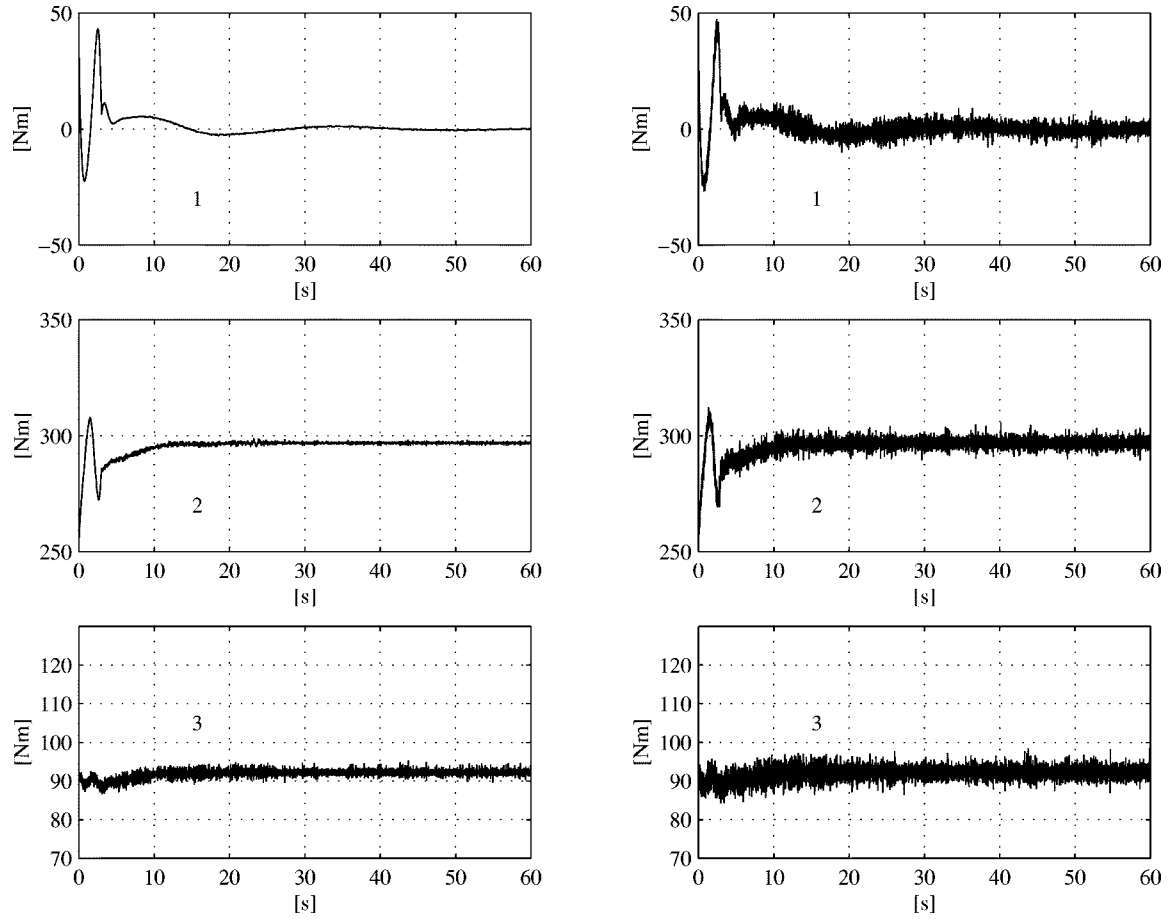

Fig. 6. Comparison of the control laws (38), (39), and (43): joint control torques. Left: control laws (38) and (39); Right: control law (43). The third torque, due to the smaller inertia, is the only component that shows some chattering also in the controller-observer scheme.

A digital implementation of the control laws has been considered. The sensor update rate is 100 Hz for the joint positions and 20 Hz for the vehicle position and orientation, while the control inputs to the actuators are updated at 100 Hz, i.e., the control law is computed every 10 ms. The relatively high update rate for the vehicle position and orientation measurements has been chosen so as to achieve a satisfactory tracking accuracy. Of course, such update rates can be obtained if high-performance sensors, e.g., video systems, are available.

Quantization effects have been introduced into the simulation by assuming a 16-bit A/D converter on the sensors outputs. Also, Gaussian zero-mean noise has been added to the signals coming from the sensors.

Fig. 3 shows the time history of the norm of the tracking and estimation errors obtained with the control laws (38), (39), and (43), respectively. Figs. 4–6 show the corresponding control forces, moments, and torques. It can be recognized that good tracking is achieved in both cases, although the performance in terms of tracking error is slightly better for the control law (43), where numerical derivatives are used. On the other hand, the presence of measurement noise and quantization effects results in chattering of the control commands to the actuators; this is much lower when the control laws (38) and (39) are adopted than with control law (43). An indicator of the energy consumption due to the chattering at steady state is the variance of the control commands reported in Table II for each component; these data clearly show the advantage of using the controller-observer scheme. Of course, the improvement becomes clear when the noise and quantization effects are larger than a certain threshold. The derivation of such a threshold would require a stochastic analysis of a nonlinear system, which is beyond the scope of this work. Moreover, it can be easily recognized that such a bound is strongly dependent on the characteristics of the actuators.

TABLE II
VARIANCE OF CONTROL COMMANDS

	Control law (38),(39)	Control law (43)
Force x [N^2]	0.0149	14.6326
Force y [N^2]	0.0077	11.4734
Force z [N^2]	0.0187	3.0139
Moment x [N^{2}m^2]	0.2142	10.6119
Moment y [N^{2}m^2]	2.8156	23.2798
Moment z [N^{2}m^2]	1.6192	26.0350
Torque 1 [N^{2}m^2]	0.3432	4.0455
Torque 2 [N^{2}m^2]	0.0725	3.2652
Torque 3 [N^{2}m^2]	0.3393	1.8259

B. Second Case Study

In this case study, the same task as above is executed by adopting the control law (40) and (41) and its counterpart using

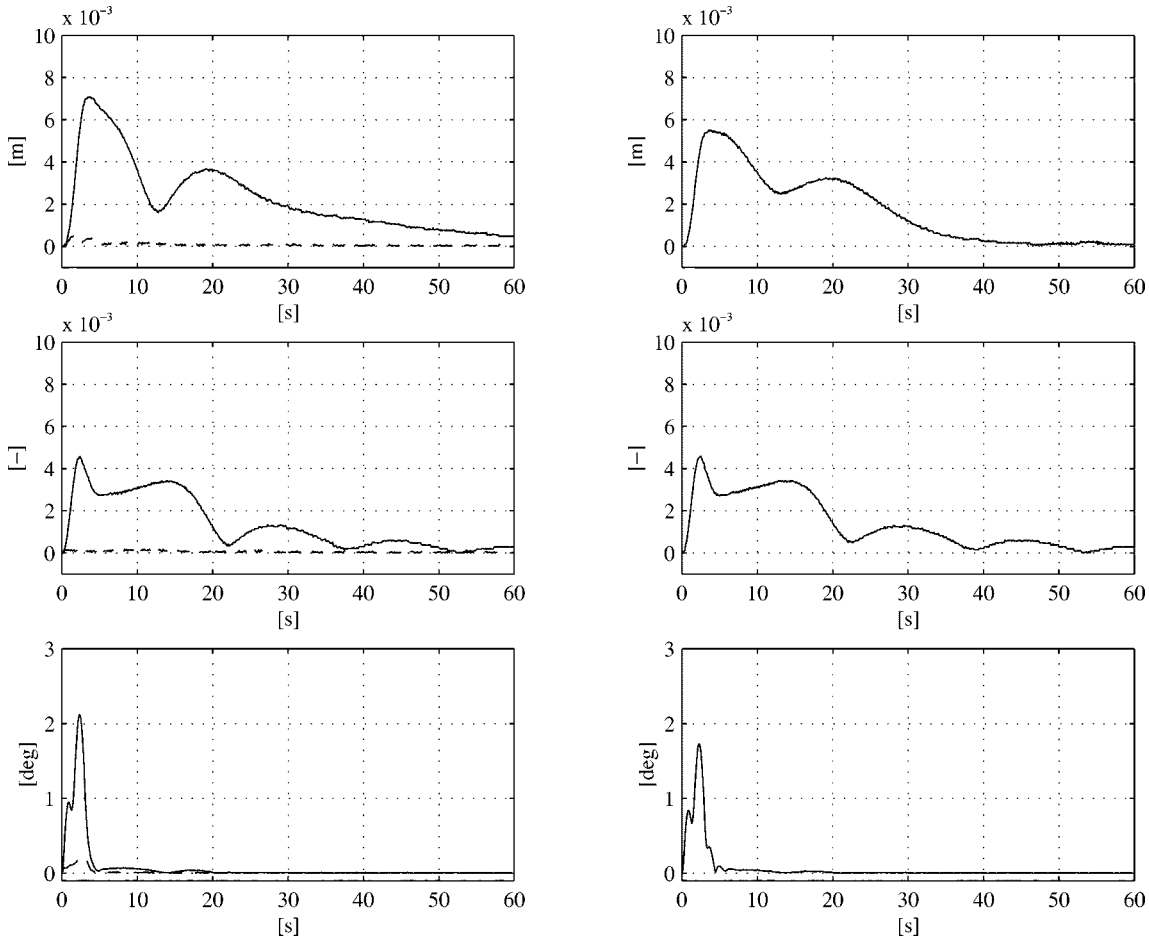

Fig. 7. Comparison of the control laws (40), (41), and (44): norm of the tracking (solid line) and estimation (dashed line) errors. Top: vehicle position error. Middle: vehicle orientation error (vector part of the quaternion). Bottom: joint position errors. Notice that the performance in terms of the tracking error is still good using the reduced versions of the controller-observer scheme and of the law obtained using the numerical differentiation.

numerical differentiation of the measured position/orientation, i.e.,

$$\mathbf{u} = \mathbf{B}^{\dagger}(\hat{\mathbf{M}}\dot{\boldsymbol{\zeta}}_r + \mathbf{K}_v(\boldsymbol{\zeta}_r - \boldsymbol{\zeta}) + \mathbf{K}_p\mathbf{e}_d + \mathbf{g}(\mathbf{q}, \mathbf{R}^0)) \quad (44)$$

where the same parameters as in the previous case study have been used. Also, the same measurement update rates, quantization resolution, and sensory noise have been considered in the simulation.

The results are reported in Fig. 7 in terms of tracking and estimation errors. It can be recognized that the errors are comparable to those obtained with the control scheme (38) and (39) in spite of the extremely simplified control structure; also, the control inputs remain free of chattering phenomena and are not reported for the sake of brevity.

The tracking performance obtained with the simplified control law confirms that the controller-observer approach is intrinsically robust with respect to uncertain knowledge of the system's dynamics, thanks to the exponential stability property. Hence, perfect compensation of inertia, Coriolis, and centripetal terms, as well as of hydrodynamic damping terms, is not required.

C. Third Case Study

The control laws (40), (41), and (44) have been tested under severe operating conditions. Namely, the update rate for the vehicle position/orientation measurements has been lowered to 5 Hz and the A/D word length has been set to 12 bit for all the sensor output signals. Gaussian zero-mean noise is still added to the measures. The parameters in the control laws are the same as in the previous case studies.

Fig. 8 shows a small degradation of the tracking performance for both the control schemes. In fact, the tracking errors remain the same order of magnitude as in the previous case studies, because the computing rate of the control law is unchanged (100 Hz). Namely, the update rate of the measurements relative to the subsystem with faster dynamics (i.e., the manipulator) remains the same (100 Hz), while the update rate of the measurements relative to the vehicle (5 Hz) is still adequate to its slower dynamics. Figs. 9–11 show the corresponding control forces, moments, and torques. It can be recognized that unacceptable chattering on the control inputs is experienced when numerical derivatives are used, which is almost completely canceled when the controller-observer scheme is adopted.

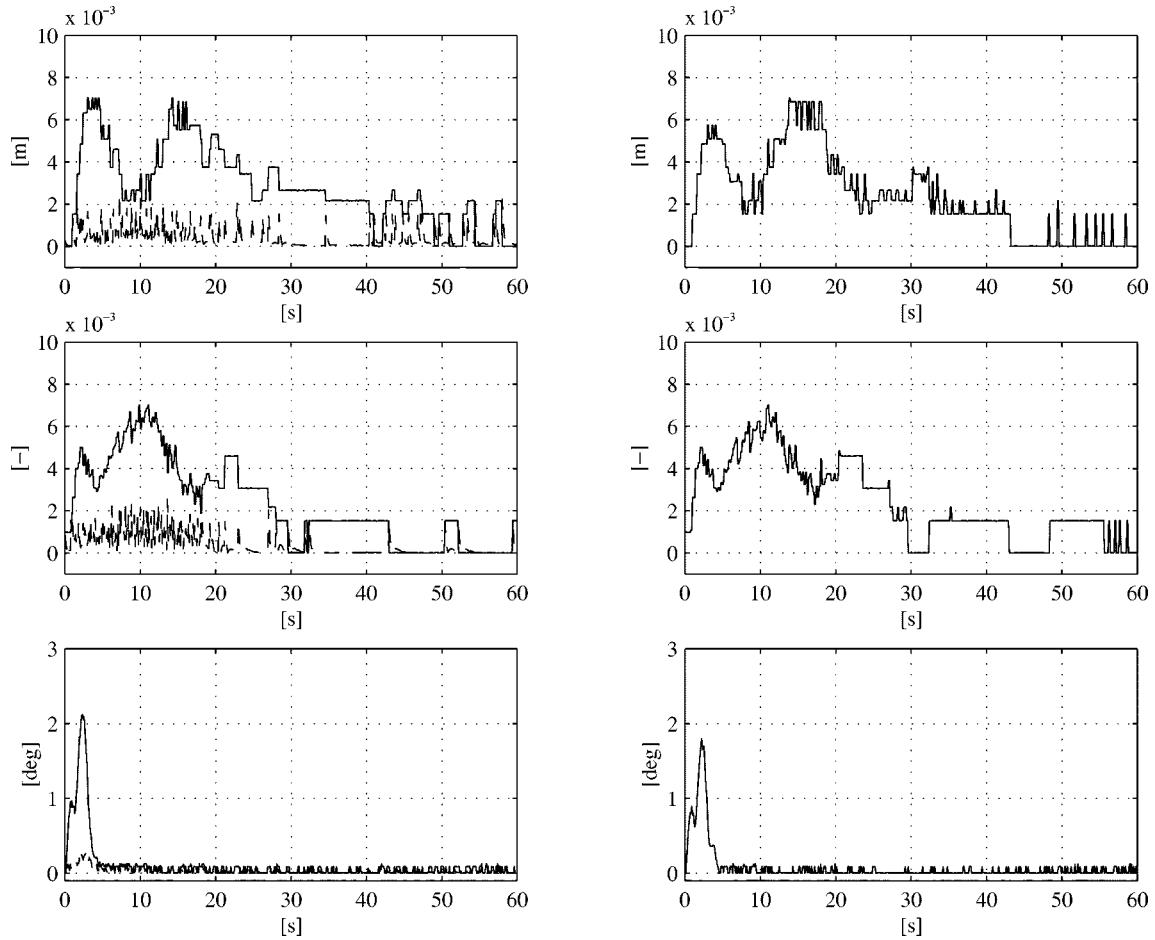

Fig. 8. Comparison between the control laws (40), (41) and (44): norm of the tracking (solid) and estimation (dashed) errors. Left: control law (40), (41). Right: control law (44). Top: vehicle position error; Middle: vehicle orientation error (vector part of the quaternion); Bottom: joint position errors. In case of smaller sampling time and word length both the control laws guarantee satisfactory tracking errors for the vehicle position/orientation, an increase of the errors is observed for the manipulator variables.

VIII. Conclusions

In this paper, a new control law for tracking of a desired motion trajectory for an underwater vehicle-manipulator system has been proposed. A novel observer has been designed to provide estimation of velocities used by the control law. It has been proven that the resulting controller-observer scheme achieves exponential convergence to zero of both motion tracking and estimation errors. Moreover, representation singularities of the orientation are avoided thanks to the use of unit quaternions. Simulation results show the effectiveness of the proposed controller-observer algorithm when compared to the performance achieved with a control scheme using numerically reconstructed velocities. In fact, the use of the velocity observer allows for the reduction of chattering on the control commands due to sensory noise and quantization, and thus provides better operating conditions for the actuators, i.e., energy saving and increased lifetime. Partial compensation of inertial and hydrodynamic terms as well as low update rates and heavy quantization of sensor measurements have been considered in some case studies. The results confirm the robustness of the controller-observer scheme with regard to unmodeled dynamics and external disturbances.

Appendix
Stability Analysis

Consider the positive definite Lyapunov function candidate

$$\begin{aligned} V = {} & \frac{1}{2}\boldsymbol{\sigma}_d^T\mathbf{M}(\mathbf{q})\boldsymbol{\sigma}_d + \frac{1}{2}\boldsymbol{\sigma}_e^T\mathbf{M}(\mathbf{q})\boldsymbol{\sigma}_e + \frac{1}{2}k_{pP}\tilde{\mathbf{p}}_d^T\tilde{\mathbf{p}}_d \\ & + k_{pO}\left((1-\tilde{\eta}_d)^2 + \tilde{\boldsymbol{\epsilon}}_d^T\tilde{\boldsymbol{\epsilon}}_d\right) + \frac{1}{2}\tilde{\mathbf{q}}_d^T\mathbf{K}_{pQ}\tilde{\mathbf{q}}_d \\ & + \frac{1}{2}l_{pP}\tilde{\mathbf{p}}_e^T\tilde{\mathbf{p}}_e + l_{pO}\left((1-\tilde{\eta}_e)^2 + \tilde{\boldsymbol{\epsilon}}_e^T\tilde{\boldsymbol{\epsilon}}_e\right) + \frac{1}{2}\tilde{\mathbf{q}}_e^T\mathbf{L}_{pQ}\tilde{\mathbf{q}}_e. \end{aligned} \tag{45}$$

The time derivative of V along the trajectories of the closed-loop system (35) and (36) is given by

$$\begin{aligned} \dot{V} = {} & -\boldsymbol{\sigma}_d^T\mathbf{K}_v\boldsymbol{\sigma}_d - \mathbf{e}_{de}^T\boldsymbol{\Lambda}_d\mathbf{K}_p\mathbf{e}_d - \mathbf{e}_e^T\boldsymbol{\Lambda}_e\mathbf{L}_p\mathbf{e}_e \\ & - \boldsymbol{\sigma}_e^T(\mathbf{L}_v\mathbf{A}(\tilde{\mathcal{Q}}_e) - \mathbf{K}_v)\boldsymbol{\sigma}_e - \boldsymbol{\sigma}_d^T\mathbf{C}(\mathbf{q},\boldsymbol{\sigma}_e)\boldsymbol{\zeta}_r \\ & - \boldsymbol{\sigma}_e^T\mathbf{C}(\mathbf{q},\boldsymbol{\zeta})\boldsymbol{\sigma}_e + \boldsymbol{\sigma}_e^T\mathbf{C}^T(\mathbf{q},\boldsymbol{\sigma}_d)\boldsymbol{\zeta}_o + (\boldsymbol{\sigma}_d+\boldsymbol{\sigma}_e)^T \\ & \times \mathbf{D}(\mathbf{q},\boldsymbol{\zeta})\boldsymbol{\zeta} - \frac{1}{2}(\boldsymbol{\sigma}_d+\boldsymbol{\sigma}_e)^T\mathbf{D}(\mathbf{q},\boldsymbol{\zeta}_r)(\boldsymbol{\zeta}_r+\boldsymbol{\zeta}_o) \\ & - \boldsymbol{\sigma}_d^T\mathbf{M}(\mathbf{q})\mathbf{S}_{PO}(\tilde{\boldsymbol{\omega}}_d)\boldsymbol{\zeta}_d - \boldsymbol{\sigma}_d^T\mathbf{M}(\mathbf{q})\boldsymbol{\Lambda}_d\mathbf{S}_P(\tilde{\boldsymbol{\omega}}_d)\mathbf{e}_{de}. \end{aligned} \tag{46}$$

In the following it is assumed that $\tilde{\eta}_d > 0, \tilde{\eta}_e > 0$; in view of the angle/axis interpretation of the unit quaternion, the above

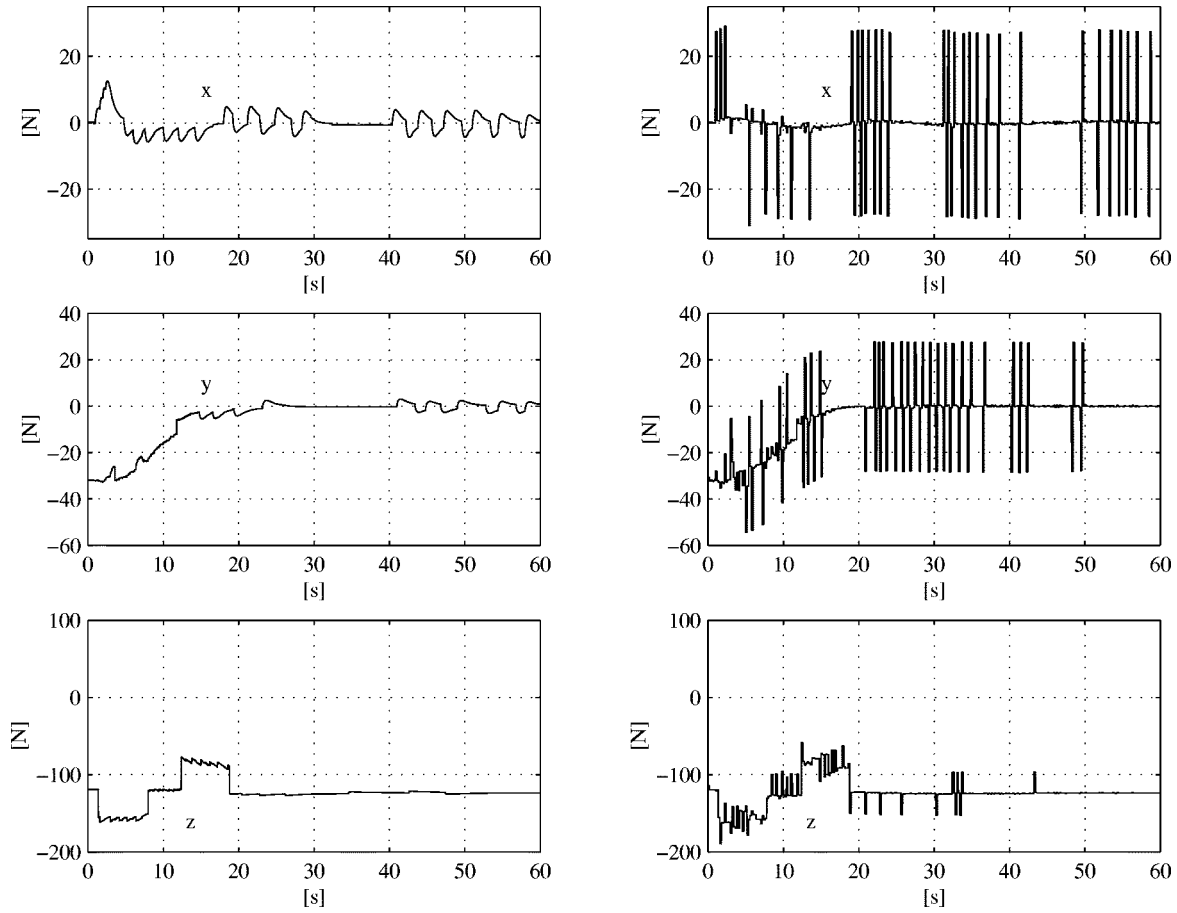

Fig. 9. Comparison of the control laws (40), (41), and (44): vehicle control forces. Left: control laws (40) and (41). Right: control law (44). The controller-observer scheme (left) is working at a low frequency without causing chattering to the control inputs, as is the case with the numerical derivatives scheme (right).

assumption corresponds to considering orientation errors characterized by angular displacements in the range $]-\pi,\pi[$.

From the equality $\tilde{\mathcal{Q}}_{de} = \tilde{\mathcal{Q}}_e^{-1} * \tilde{\mathcal{Q}}_d$, the following equality results:

$$\tilde{\epsilon}_{de}^{eT}\tilde{\epsilon}_d = \tilde{\eta}_e\tilde{\epsilon}_d^T\tilde{\epsilon}_d - \tilde{\eta}_d\tilde{\epsilon}_d^T\tilde{\epsilon}_e$$

where $\tilde{\eta}_d$ and $\tilde{\eta}_e$ are the scalar parts of the quaternions $\tilde{\mathcal{Q}}_d$ and $\tilde{\mathcal{Q}}_e$, respectively. The above equation, in view of $\tilde{\mathbf{p}}_{de} = \tilde{\mathbf{p}}_d - \tilde{\mathbf{p}}_e$ and $\tilde{\mathbf{q}}_{de} = \tilde{\mathbf{q}}_d - \tilde{\mathbf{q}}_e$, implies that

$$\begin{aligned}\mathbf{e}_{de}^T\mathbf{\Lambda}_d\mathbf{K}_p\mathbf{e}_d = {} & k_{pP}\tilde{\mathbf{p}}_d^T\mathbf{\Lambda}_{dP}\tilde{\mathbf{p}}_d + \lambda_{dO}k_{pO}\tilde{\eta}_e\|\tilde{\epsilon}_d\|^2 \\ & + \tilde{\mathbf{q}}_d^T\mathbf{\Lambda}_{dQ}\mathbf{K}_{pQ}\tilde{\mathbf{q}}_d - k_{pP}\tilde{\mathbf{p}}_d^T\mathbf{\Lambda}_{dP}\tilde{\mathbf{p}}_e \\ & - \lambda_{dO}k_{pO}\tilde{\eta}_d\tilde{\epsilon}_d^T\tilde{\epsilon}_e + \tilde{\mathbf{q}}_d^T\mathbf{\Lambda}_{dQ}\mathbf{K}_{pQ}\tilde{\mathbf{q}}_e\end{aligned}$$

and thus

$$\mathbf{e}_{de}^T\mathbf{\Lambda}_d\mathbf{K}_p\mathbf{e}_d \geq k_{pm}\tilde{\eta}_e\|\mathbf{e}_d\|^2 - k_{pM}\|\mathbf{e}_d\|\|\mathbf{e}_e\| \qquad (47)$$

where k_{pm} (k_{pM}) is the minimum (maximum) eigenvalue of the matrix $\mathbf{\Lambda}_d\mathbf{K}_p$. Moreover, in view of the block diagonal structure of the matrix $\mathbf{L}_v$ and of the skew-symmetry of the matrix $\mathbf{S}(\cdot)$, the following inequality holds:

$$\boldsymbol{\sigma}_e^T\mathbf{L}_v\mathbf{A}(\tilde{\mathcal{Q}}_e)\boldsymbol{\sigma}_e \geq \frac{1}{2}l_{vm}\tilde{\eta}_e\|\boldsymbol{\sigma}_e\|^2 \qquad (48)$$

where l_{vm} is the minimum eigenvalue of the matrix $\mathbf{\Lambda}_v$.

Moreover, the last two terms in (47) can be rewritten as

$$\begin{aligned}&(\boldsymbol{\sigma}_d+\boldsymbol{\sigma}_e)^T\mathbf{D}(\mathbf{q},\boldsymbol{\zeta})\boldsymbol{\zeta} - \frac{1}{2}(\boldsymbol{\sigma}_d+\boldsymbol{\sigma}_e)^T\mathbf{D}(\mathbf{q},\boldsymbol{\zeta}_r)(\boldsymbol{\zeta}_r+\boldsymbol{\zeta}_o) \\ &\quad = -\frac{1}{2}(\boldsymbol{\sigma}_d+\boldsymbol{\sigma}_e)^T\mathbf{D}(\mathbf{q},\boldsymbol{\zeta})(\boldsymbol{\sigma}_d+\boldsymbol{\sigma}_e) \\ &\qquad - \frac{1}{2}(\boldsymbol{\sigma}_d+\boldsymbol{\sigma}_e)^T(\mathbf{D}(\mathbf{q},\boldsymbol{\zeta}_r) - \mathbf{D}(\mathbf{q},\boldsymbol{\zeta}))(\boldsymbol{\zeta}_r+\boldsymbol{\zeta}_o). \qquad (49)\end{aligned}$$

In view of properties 1–3 and (30), (31), (47), and (48), by taking into account that $\boldsymbol{\zeta} = \boldsymbol{\zeta}_d - \tilde{\boldsymbol{\zeta}}_d$ with $\|\boldsymbol{\zeta}_d\| \leq \zeta_{dM}$ and $\|\mathbf{e}_{de}\| \leq \|\mathbf{e}_d\| + \|\mathbf{e}_e\|$, the function $\dot{V}$ can be upper bounded as follows:

$$\begin{aligned}\dot{V} \leq {} & -k_{vm}\|\boldsymbol{\sigma}_d\|^2 - k_{pm}\tilde{\eta}_e\|\mathbf{e}_d\|^2 - \frac{l_{vm}}{2}\tilde{\eta}_e\|\boldsymbol{\sigma}_e\|^2 \\ & + k_{vM}\|\boldsymbol{\sigma}_d\|^2 - l_{pm}\|\mathbf{e}_e\|^2 + k_{pM}\|\mathbf{e}_d\|\|\mathbf{e}_e\| \\ & + C_M\|\boldsymbol{\sigma}_d\|\|\boldsymbol{\sigma}_e\|(2\|\tilde{\boldsymbol{\zeta}}_d\| + 2\zeta_{dM} + \|\boldsymbol{\sigma}_d\| + \|\boldsymbol{\sigma}_e\|) \\ & + C_M\|\boldsymbol{\sigma}_e\|^2(\|\tilde{\boldsymbol{\zeta}}_d\| + \zeta_{dM}) + \frac{D_M}{2}(\|\boldsymbol{\sigma}_d\|^2 + \|\boldsymbol{\sigma}_d\|\|\boldsymbol{\sigma}_e\|) \\ & \times (2\|\tilde{\boldsymbol{\zeta}}_d\| + 2\zeta_{dM} + \|\boldsymbol{\sigma}_d\| + \|\boldsymbol{\sigma}_e\|) \\ & + M_M\|\boldsymbol{\sigma}_d\|\|\tilde{\boldsymbol{\zeta}}_d\|(\zeta_{dM} + \lambda_{dM}(\|\mathbf{e}_d\| + \|\mathbf{e}_e\|)) \qquad (50)\end{aligned}$$

where k_{vm} (k_{vM}) denotes the minimum (maximum) eigenvalue of the matrix $\mathbf{K}_v$, l_{pm} denotes the minimum eigenvalue of $\boldsymbol{\Lambda}_e\mathbf{L}_p$, and λ_{dM} denotes the maximum eigenvalue of the matrix $\mathbf{\Lambda}_d$.

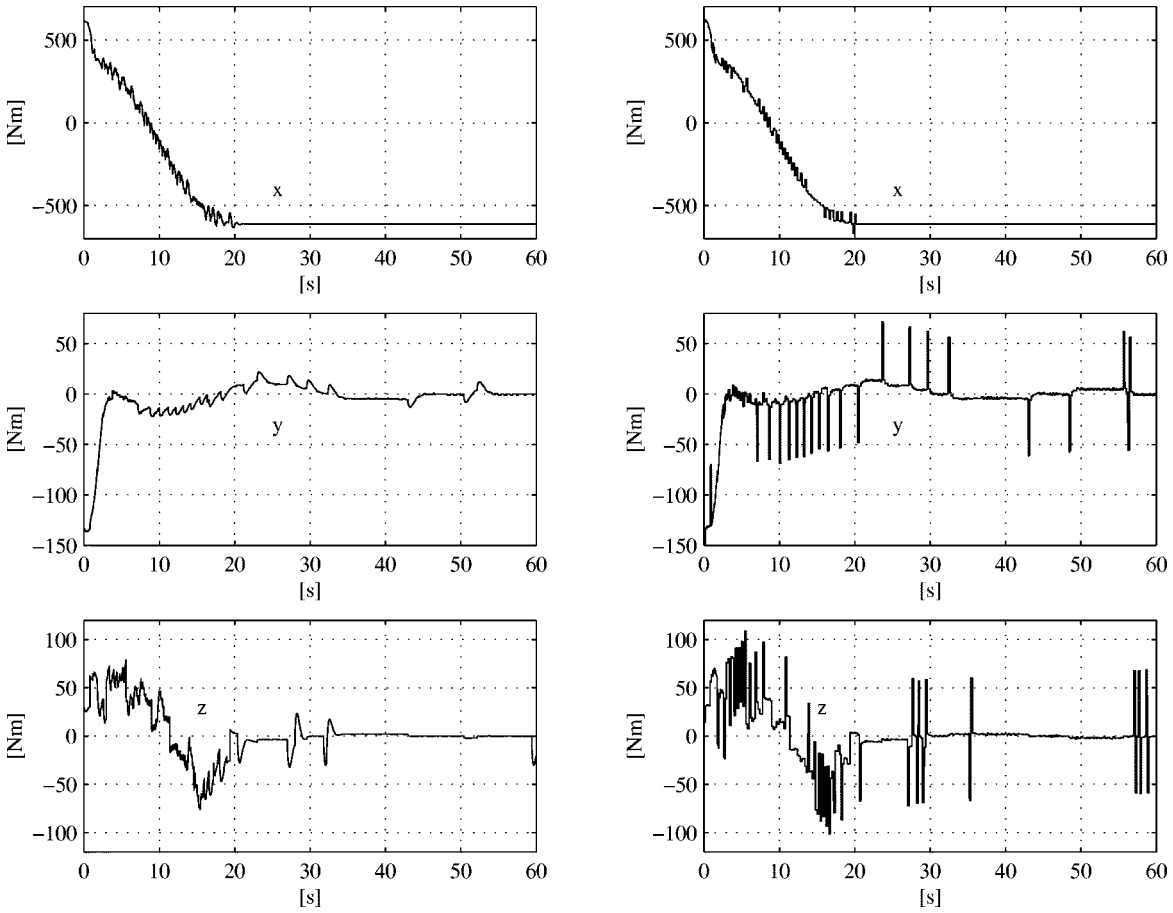

Fig. 10. Comparison of the control laws (40), (41), and (44): vehicle control moments. Left: control laws (40) and (41). Right: control law (44). Notice also that, at steady state, small displacements or measurement errors can cause intolerable control actions in the numerical derivatives scheme.

Consider the state-space domain defined as follows:

$$B_\rho = \{\mathbf{x} : \|\mathbf{x}\| < \rho,\ \rho < 1\} \tag{51}$$

with $\tilde{\eta}_d > 0, \tilde{\eta}_e > 0$. It can be recognized that, in the domain B_ρ, the following inequalities hold:

$$0 < \sqrt{1-\rho^2} < \tilde{\eta}_e < 1, \tag{52}$$

$$\|\tilde{\boldsymbol{\zeta}}_d\| = \|\boldsymbol{\sigma}_d - \boldsymbol{\Lambda}_d \mathbf{e}_{de}\| \leq (1 + 2\lambda_{dM})\rho. \tag{53}$$

By completing the squares in (50) and using (52) and (53), it can be shown that there exists a scalar $\kappa > 0$ such that

$$\dot{V} \leq -\kappa \|\mathbf{x}\|^2 \tag{54}$$

in the domain B_ρ, provided that the controller and observer parameters satisfy the inequalities

$$k_{vm} > \alpha_1 \left(C_M + \frac{3D_M}{2} \right) + \alpha_2 M_M (1 + \lambda_{dM}) \tag{55}$$

$$k_{pm} > \frac{\alpha_2 M_M \lambda_{dM}}{\sqrt{1-\rho^2}} \tag{56}$$

$$l_{pm} > \max\left\{ \alpha_2 M_M \lambda_{dM}, \frac{k_{pM}^2}{k_{pm}\sqrt{1-\rho^2}} \right\} \tag{57}$$

$$l_{vm} > \frac{2}{\sqrt{1-\rho^2}} \left(k_{vM} + (2\alpha_1 + \rho) C_M + \frac{\alpha_1 D_M}{2} \right) \tag{58}$$

where $\alpha_1 = 2(1 + \lambda_{dM})\rho + \zeta_{dM}$ and $\alpha_2 = \zeta_{dM} + 2\lambda_{dM}\rho$.

Therefore, given a domain B_ρ characterized by any $\rho < 1$, there always exists a set of observer and controller gains such that $\dot{V} \leq 0$ in B_ρ. Moreover, for $\tilde{\eta}_d \geq 0, \tilde{\eta}_e \geq 0$, the following inequality holds

$$0 \leq (1 - \tilde{\eta}_d)^2 \leq (1 - \tilde{\eta}_d)(1 + \tilde{\eta}_d) = \|\tilde{\epsilon}_d\|^2$$

and a similar inequality can be written in terms of $\tilde{\eta}_e$ and $\tilde{\epsilon}_e$. Hence, function V can be bounded as

$$c_m \|\mathbf{x}\|^2 \leq V(\mathbf{x}) \leq c_M \|\mathbf{x}\|^2 \tag{59}$$

with

$$c_m = \frac{1}{2} \min\{M_m, k'_{pm}, l'_{pm}\}$$

$$c_M = \frac{1}{2} \max\{M_M, 4k'_{pM}, 4l'_{pM}\}$$

where k'_{pm} (k'_{pM}) is the minimum (maximum) eigenvalue of the matrix $\mathbf{K}_p$, and l'_{pm} (l'_{pM}) is the minimum (maximum) eigenvalue of the matrix $\mathbf{L}_p$.

Since $V(t)$ is a decreasing function along the system trajectories, the inequality (59) guarantees that, for a given $0 < \rho < 1$, all the trajectories $\mathbf{x}(t)$ starting in the domain

$$\Omega_\rho = \left\{ \mathbf{x} : \|\mathbf{x}\| < \rho \sqrt{\frac{c_m}{c_M}} \right\} \tag{60}$$

remain in the domain B_ρ for all $t > 0$ provided that $\tilde{\eta}_d(t) > 0, \tilde{\eta}_e(t) > 0$ for all $t > 0$. The latter condition is fulfilled when

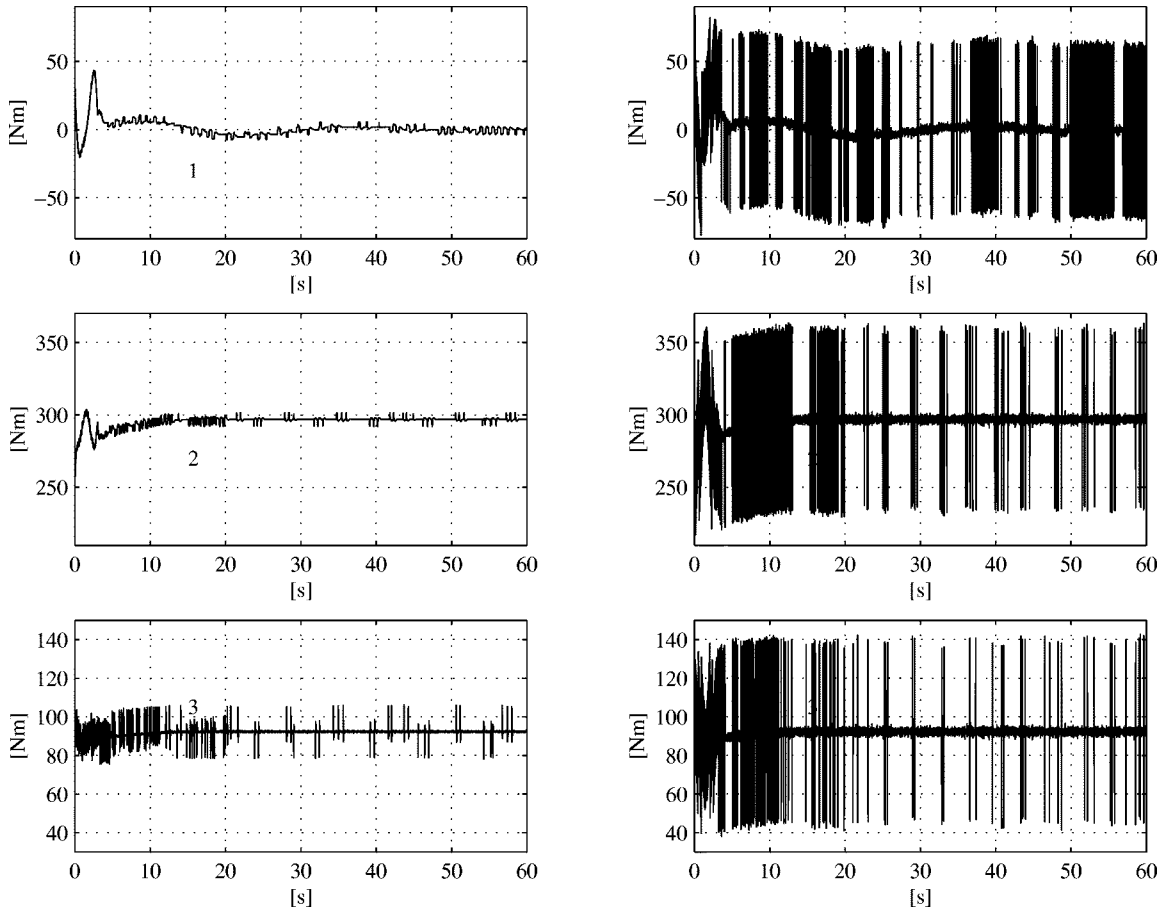

Fig. 11. Comparison of the control laws (40), (41), and (44): joint control torques. Left: control laws (40) and (41). Right: control law (44). It is worth noticing that control actions too noisy (right) would not be accepted; smaller control gains, with consequently larger tracking errors, would be designed for the numerical derivatives approach.

$\tilde{\eta}_d(0)$ and $\tilde{\eta}_e(0)$ are positive; in fact, $||\tilde{\epsilon}_d|| < \rho < 1$ and $||\tilde{\epsilon}_e|| < \rho < 1$ for all $t > 0$ implies that $\tilde{\eta}_d(t)$ and $\tilde{\eta}_e(t)$ cannot change their sign.

Moreover, from (54) and (59), the convergence in the domain B_ρ is exponential [26], which implies exponential convergence of $\mathbf{e}_d$, $\mathbf{e}_e$, $\tilde{\boldsymbol{\zeta}}_d$, and $\tilde{\boldsymbol{\zeta}}_e$.

The condition $\rho < 1$ is due to the unit norm constraint on the quaternion components and gives a rather conservative estimate of the domain of attraction. However, it must be pointed out that this limitation arises when spheres are used to estimate the domain of attraction; better estimates can be obtained by using domain of different shapes, e.g., ellipsoids.

REFERENCES

[1] I. Schjølberg and T. I. Fossen, "Modeling and control of underwater vehicle-manipulator systems," in *Proc. 3rd Conf. Marine Craft Maneuvering and Control*, Southampton, U.K., 1994, pp. 45–57.

[2] C. C. de Wit, E. O. Diaz, and M. Perrier, "Control of underwater vehicle/manipulator with composite dynamics," in *Proc. American Control Conf.*, Philadelphia, PA, 1998, pp. 389–393.

[3] G. Antonelli, F. Caccavale, and S. Chiaverini, "A modular scheme for adaptive control of underwater vehicle-manipulator systems," in *Proc. 1999 American Control Conf.*, San Diego, CA, 1999, pp. 3008–3012.

[4] T. Fossen and J. Balchen, "The NEROV autonomous underwater vehicle," in *Proc. OCEANS'91 Conf.*, Honolulu, HI, 1991.

[5] T. Fossen and O. Fjellstad, "Robust adaptive control of underwater vehicles: A comparative study," in *Proc. IFAC Workshop on Control Applications in Marine Systems*, 1995.

[6] F. Lizarralde, J. T. Wen, and L. Hsu, "Quaternion-based coordinated control of a subsea mobile manipulator with only position measurements," in *Proc. 34th Conf. Decision and Control*, New Orleans, LA, 1995, pp. 3996–4001.

[7] G. Antonelli and S. Chiaverini, "Singularity-free regulation of underwater vehicle-manipulator systems," in *Proc. 1998 American Control Conf.*, Philadelphia, PA, 1998, pp. 399–403.

[8] H. Berghuis and H. Nijmeijer, "A passivity approach to controller-observer design for robots," *IEEE Trans. Robot. Automat.*, vol. 9, pp. 740–754, 1993.

[9] A. J. Healey and D. Lienard, "Multivariable sliding mode control for autonomous diving and steering of unmanned underwater vehicles," *IEEE J. Oceanic Eng.*, vol. 18, pp. 327–339, 1993.

[10] R. M. Murray, Z. Li, and S. S. Sastry, *A Mathematical Introduction to Robotic Manipulation*. Boca Raton, FL: CRC Press, 1994.

[11] O. M. Faltinsen, *Sea Loads on Ships and Offshore Structures*, Cambridge, U.K.: Cambridge Univ. Press, 1990.

[12] T. Fossen, *Guidance and Control of Ocean Vehicles*, Chichester, U.K.: Wiley, 1994.

[13] J. Yuh, "Modeling and control of underwater robotic vehicles," *IEEE Trans. Syst., Man, Cybern.*, vol. 20, pp. 1475–1483, 1990.

[14] T. W. McLain and S. M. Rock, "Development and experimental validation of an underwater manipulator hydrodynamic model," *Int. J. Robot. Res.*, vol. 17, pp. 748–759, 1998.

[15] A. J. Healey, S. M. Rock, S. Cody, D. Miles, and J. P. Brown, "Toward an improved understanding of thruster dynamics for underwater vehicles," *IEEE J. Oceanic Eng.*, vol. 20, pp. 354–361, 1995.

[16] D. R. Yoerger, J. G. Cooke, and J.-J. Slotine, "The influence of thruster dynamics on underwater vehicle behavior and their incorporation into control system design," *IEEE J. Oceanic Eng.*, vol. 15, pp. 167–178, 1990.

[17] R. E. Roberson and R. Schwertassek, *Dynamics of Multibody Systems*. Berlin, Germany: Springer-Verlag, 1988.

[18] J. C. K. Chou, "Quaternion kinematic and dynamic differential equations," *IEEE Trans. Robot. Automat.*, vol. 8, pp. 53–64, 1992.
[19] S. W. Shepperd, "Quaternion from rotation matrix," *AIAA J. Guidance Control*, vol. 1, pp. 223–224, 1978.
[20] G. Antonelli and S. Chiaverini, "Task-priority redundancy resolution for underwater vehicle-manipulator systems," in *Proc. 1998 IEEE Int. Conf. Robotics Automation*, Leuven, Belgium, 1998, pp. 768–773.
[21] ——, "Adaptive tracking control of underwater vehicle-manipulator systems," in *Proc. 1998 Int. Conf. Control Applications*, Trieste, Italy, 1998, pp. 1089–1093.
[22] H. Mahesh, J. Yuh, and R. Lakshmi, "A coordinated control of an underwater vehicle and robotic manipulator," *J. Robotic Syst.*, vol. 8, pp. 339–370, 1998.
[23] G. Antonelli and S. Chiaverini, "SIMURV. A simulation package for underwater vehicle-manipulator systems," in *3rd IMACS Symp. Mathematical Modeling*, Wien, Austria, 2000, pp. 533–536.
[24] J.-J. E. Slotine and W. Li, "Adaptive strategies in constrained manipulation," in *Proc. 1987 Int. Conf. Robotics and Automation*, Raleigh, NC, 1987, pp. 595–601.
[25] O. Egeland and J.-M. Godhavn, "Passivity-based adaptive attitude control of a rigid spacecraft," *IEEE Trans. Automat. Contr.*, vol. 39, pp. 842–846, 1994.
[26] H. K. Khalil, *Nonlinear Systems*, 2nd ed. Upper Saddle River, NJ: Prentice-Hall, 1996.

Gianluca Antonelli was born in Rome, Italy, in 1970. He received the Laurea degree in electronic engineering and the Research Doctorate degree in electronic engineering and computer science from University of Naples, Naples, Italy, in 1995 and 2000, respectively.

Since then, he has been with the University of Cassino, Cassino, Italy, where he is currently a Post-Doctoral Fellow. He was a Visiting Scholar with the Université Catholique de Louvain, CESAME, Louvain-la-Neuve, Belgium, from April to July 1996, with the Katholieke Universiteit Leuven, Division PMA, Heverlee (Leuven), Belgium, from September to December 1996, and with the University of Hawaii at Manoa, Autonomous Systems Laboratory, Honolulu, HI, from November 1998 to April 1999 . His research interests include force/motion control of robot manipulators, nonlinear control, and path planning and obstacle avoidance for autonomous underwater vehicles.

Fabrizio Caccavale was born in Naples, Italy, in 1965. He received the Laurea degree in electronic engineering and the Research Doctorate degree in electronic engineering and computer science from the University of Naples, Naples, Italy, in 1993 and 1997, respectively.

Since then, he has been with the University of Naples, where he is currently an Assistant Professor in the Department of Computer and Systems Engineering. From April to October 1996, he was a Visiting Scholar at the Department of Electrical and Computer Engineering of Rice University, Austin, TX. His research interests include manipulator inverse kinematics techniques, cooperative robot manipulation, fault diagnosis for dynamical systems, and nonlinear control of mechanical systems. He has published more than 40 journal and conference papers.

Stefano Chiaverini was born in Naples, Italy, in 1961. He received the Laurea degree and the Research Doctorate degree in electronic engineering from the University of Naples, Naples, Italy, in 1986 and 1990, respectively.

From 1990 to 1998, he was with the Department of Computer and Systems Engineering of the University of Naples. He is currently an Associate Professor of Automatic Control in the Faculty of Engineering of the University of Cassino, Cassino, Italy. His research interests include manipulator inverse kinematics techniques, redundant manipulator control, force/motion control of manipulators, cooperative robot manipulation, and underwater robotics. He has published about 100 journal and conference papers and he is co-editor of the book *Complex Robotic Systems* (London, U.K.: Springer-Verlag, 1998).

Dr. Chiaverini is currently serving as an Associate Editor of the IEEE TRANSACTIONS ON ROBOTICS AND AUTOMATION.

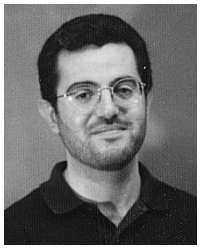

Luigi Villani was born in Avellino, Italy, in 1966. He received the Laurea degree in electronic engineering and the Research Doctorate degree in electronic engineering and computer science from the University of Naples, Naples, Italy, in 1992 and 1996, respectively.

Since then, he has been with the University of Naples, where he is currently an Assistant Professor in the Department of Computer and Systems Engineering. From June to October 1995, he was a Visiting Scholar with the Department of Automatic Control of the National Polytechnic Institute of Grenoble, France. His research interests include force/motion control of manipulators and adaptive and nonlinear control of mechanical systems. He has published about 50 journal and conference papers and is co-author of the books *Solutions Manual for Modeling and Control of Robot Manipulators* (New York: McGraw-Hill, 1996; New York: Springer, 2000, 2nd ed.) and *Robot Force Control* (Dordrecht, The Netherlands: Kluwer, 1999).

Dr. Villani is a Member of the Conference Editorial Board of the IEEE Control Systems Society.